Electronic Supporting Information

Synthesis of four regioisomeric Ni(II) azacorroles via oxidative ring-expansion of prefunctionalised norcorroles

Sha Li,[a] Shaowei Zhang,[a] Kohei Ohtake,[b] Hiroshi Shinokubo*,[b] and Xiaofang Li*,[a]

[a] Key Laboratory of Theoretical Organic Chemistry and Functional Molecules, Ministry of Education, School of Chemistry and Chemical Engineering, Hunan University of Science and Technology, Xiangtan, Hunan 411201, China

[b] Department of Molecular and Macromolecular Chemistry, Graduate School of Engineering, Research Institute for Quantum and Chemical Innovation, Institutes of Innovation for Future Society, and Integrated Research Consortium on Chemical Science (IRCCS), Nagoya University, Furo-cho, Chikusa-ku, 464-8603 Nagoya, Japan

E-mail: lixiaofang@hnust.edu.cn, hshino@chembio.nagoya-u.ac.jp

Table of contents

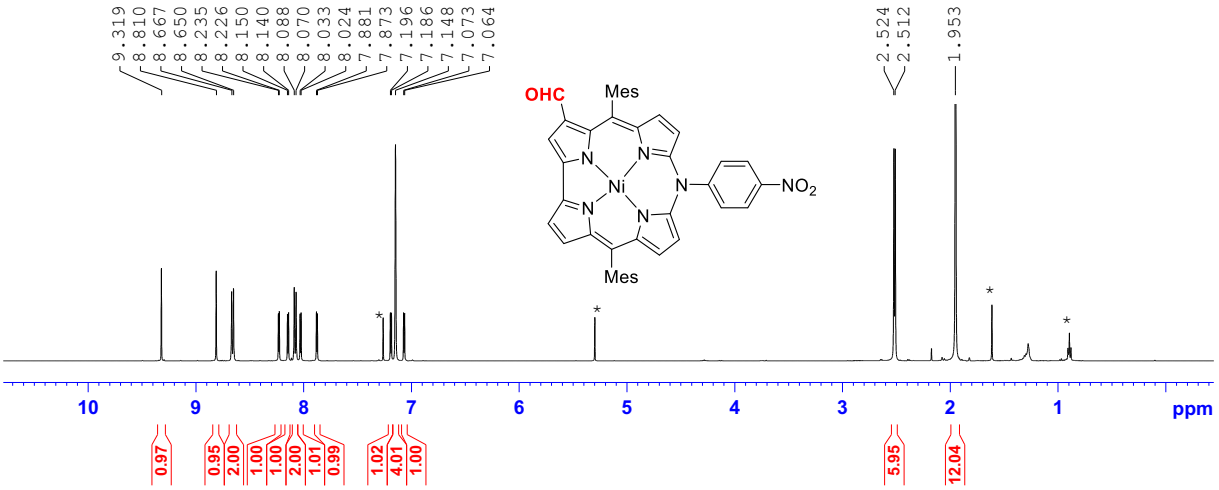

Figure S1. ^{1}H NMR spectrum of **2** (500 MHz, 298 K, $CDCl_3$).

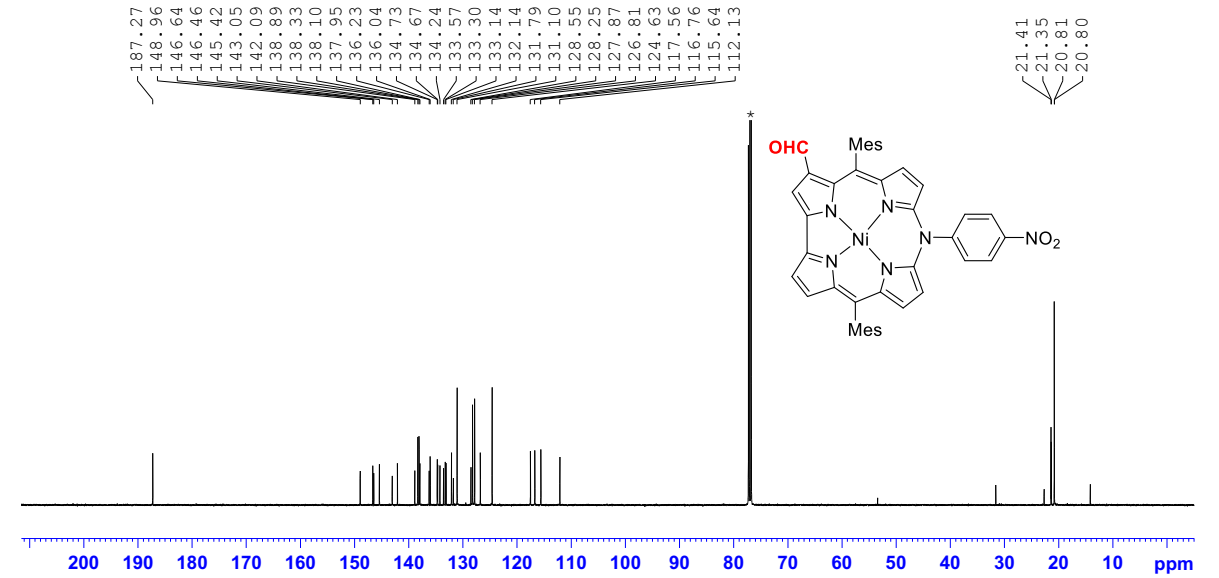

Figure S2. ^{13}C NMR spectrum of **2** (125 MHz, 298 K, $CDCl_3$).

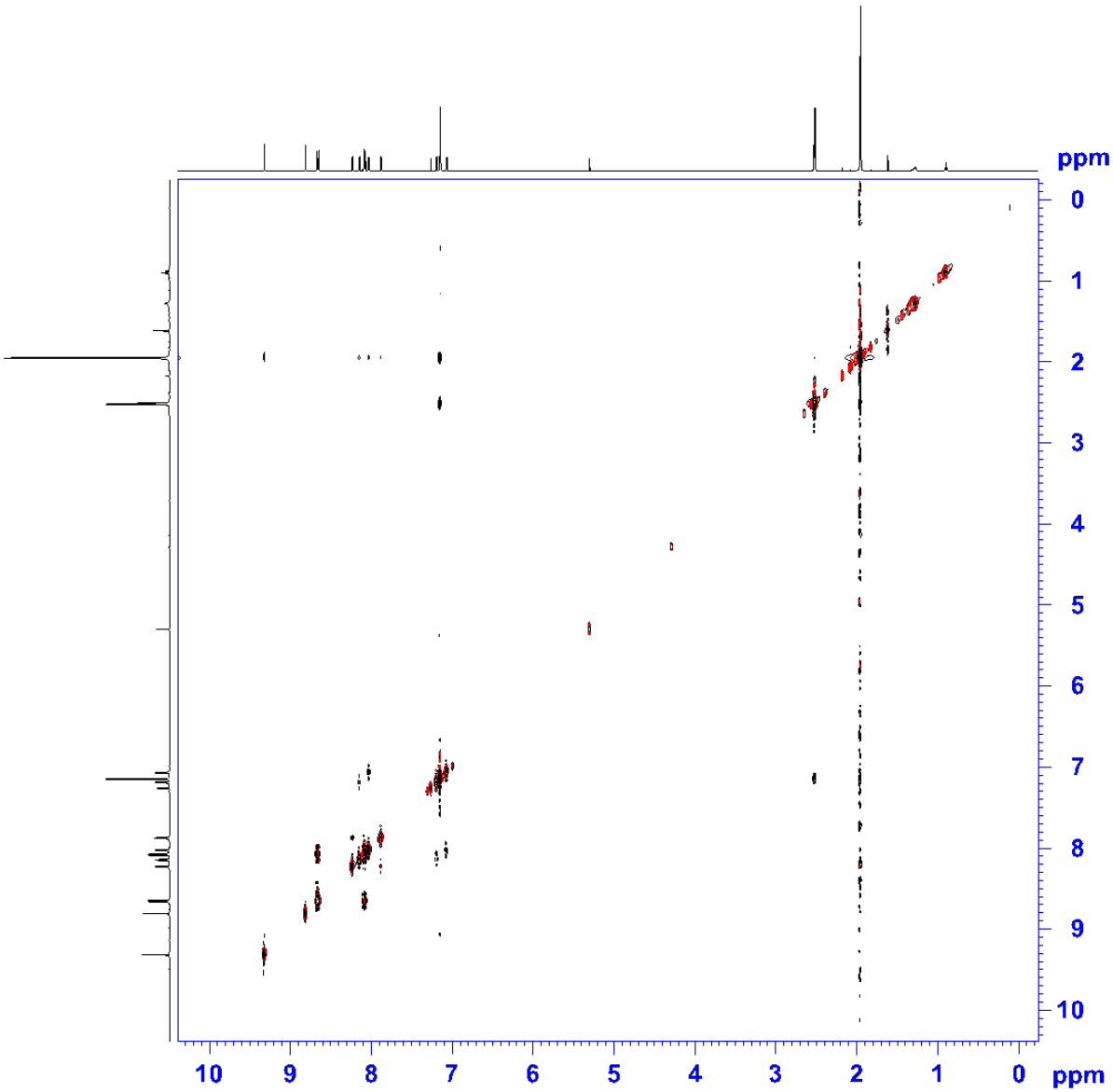

Figure S3. ^{1}H–^{1}H NOESY spectrum of **2** (500 MHz, 298 K, $CDCl_3$).

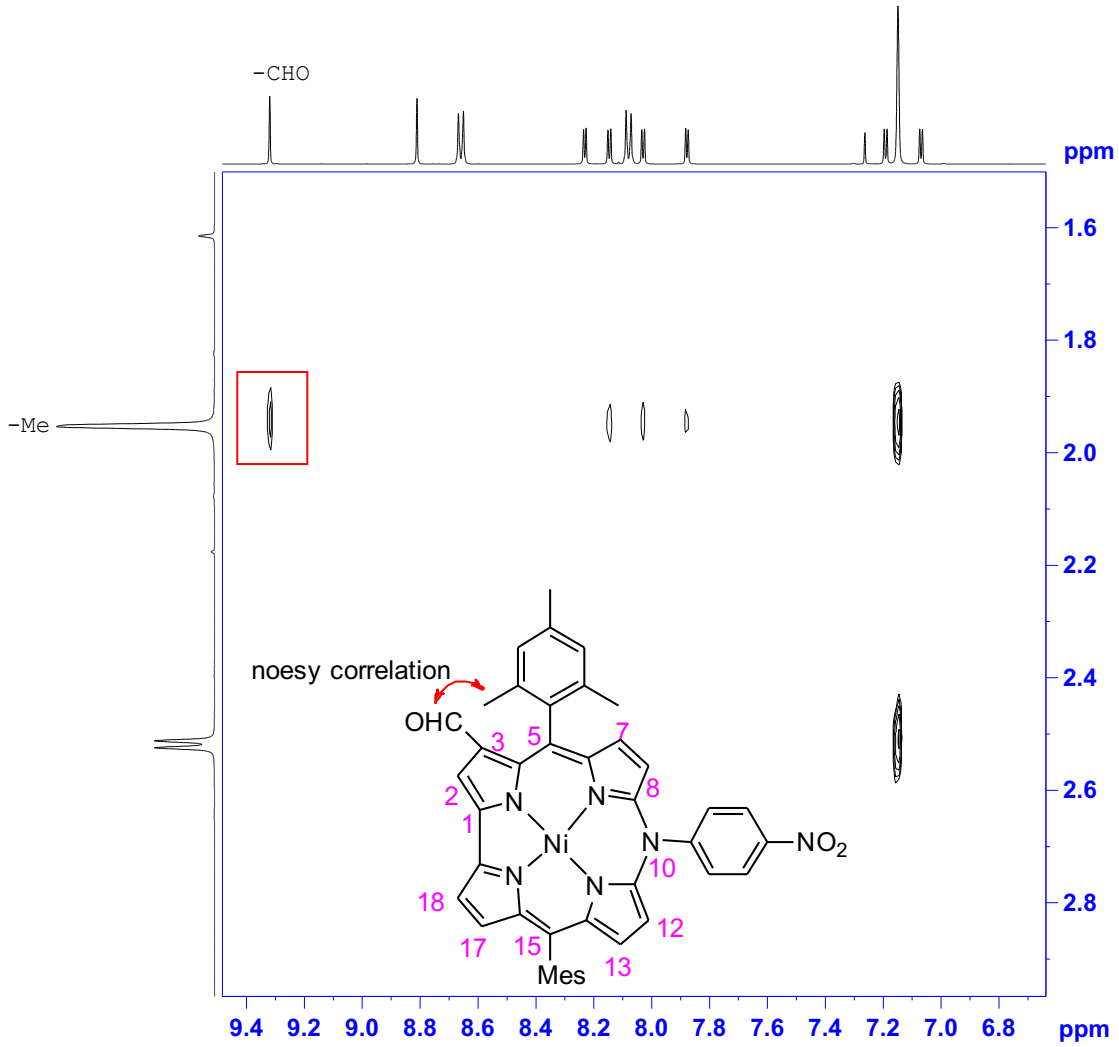

Figure S4. Magnified ^{1}H–^{1}H NOESY spectrum of **2** (500 MHz, 298 K, $CDCl_3$).

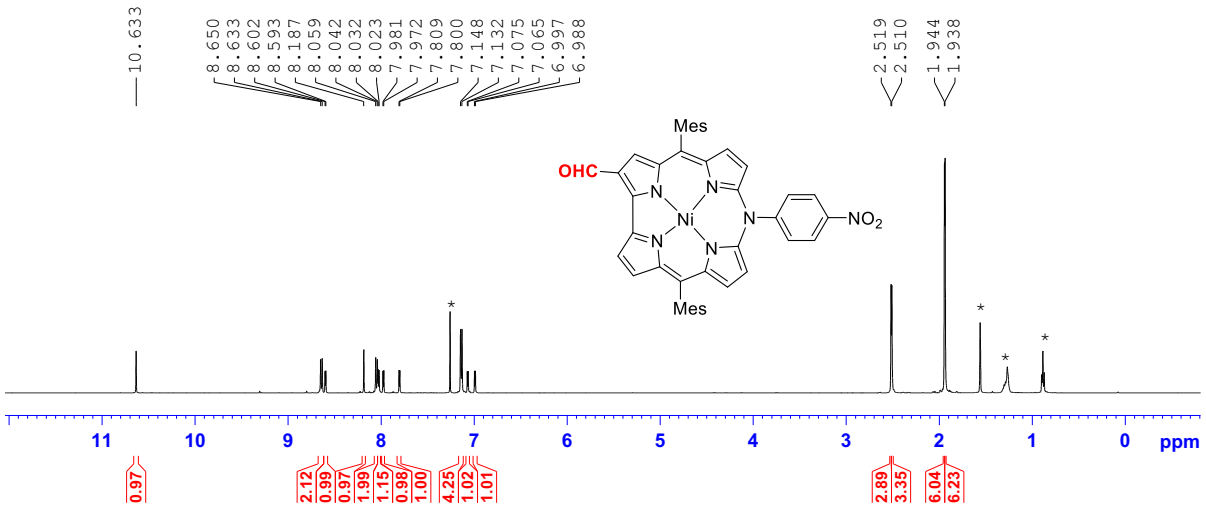

Figure S5. ^{1}H NMR spectrum of **3** (500 MHz, 298 K, $CDCl_3$).

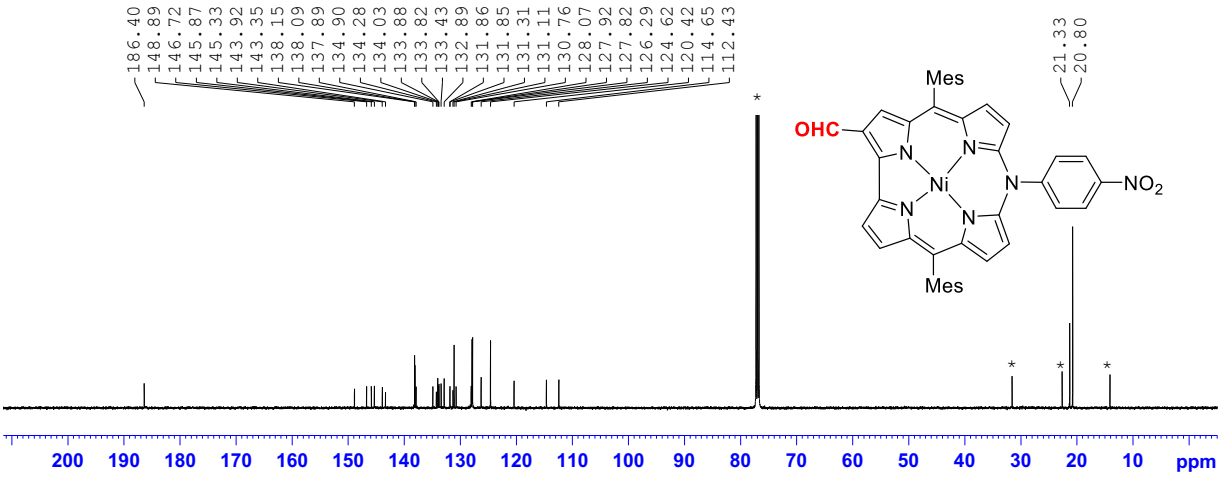

Figure S6. ^{13}C NMR spectrum of **3** (125 MHz, 298 K, $CDCl_3$).

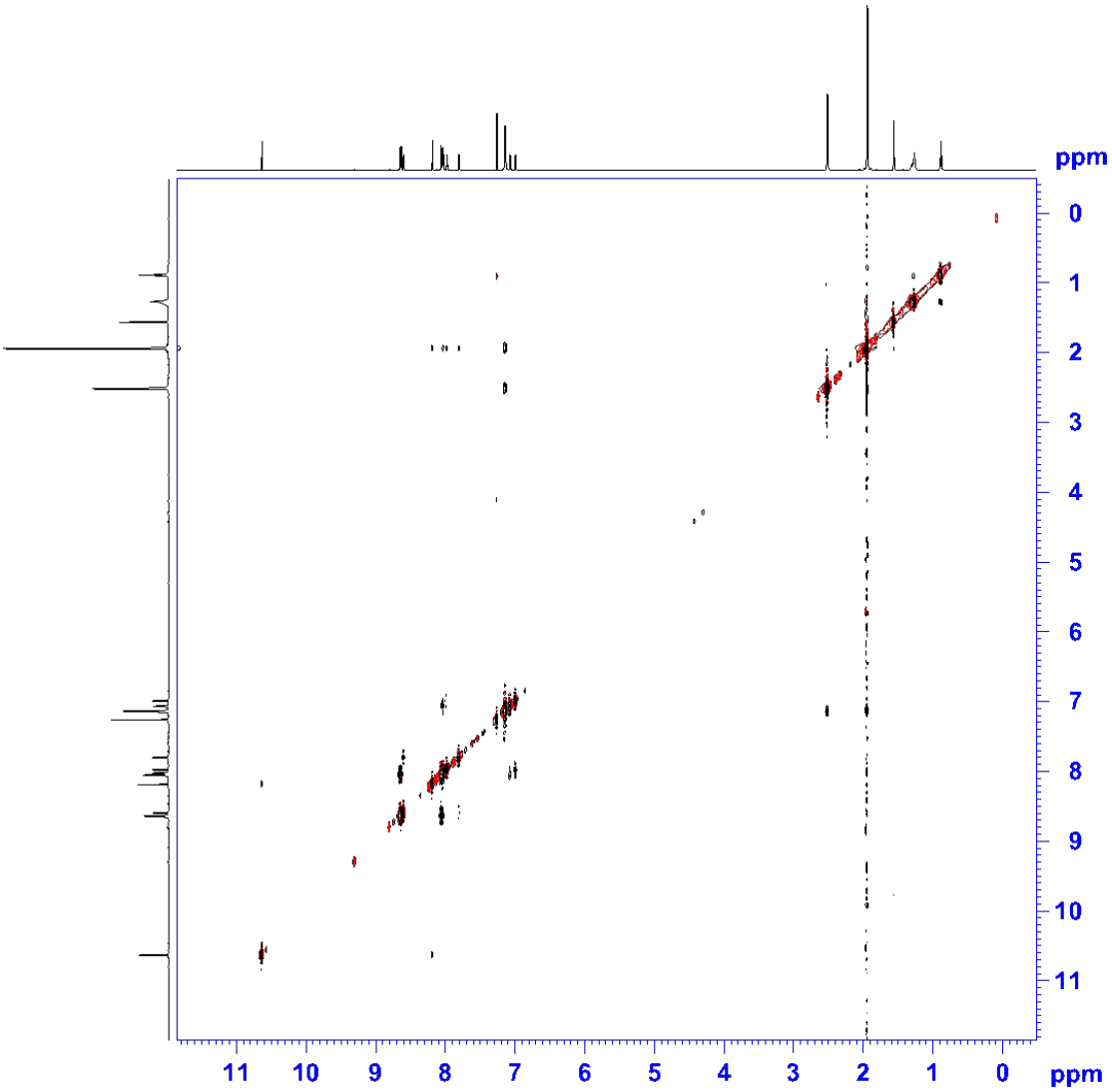

Figure S7. ^{1}H–^{1}H NOESY spectrum of **3** (500 MHz, 298 K, $CDCl_3$).

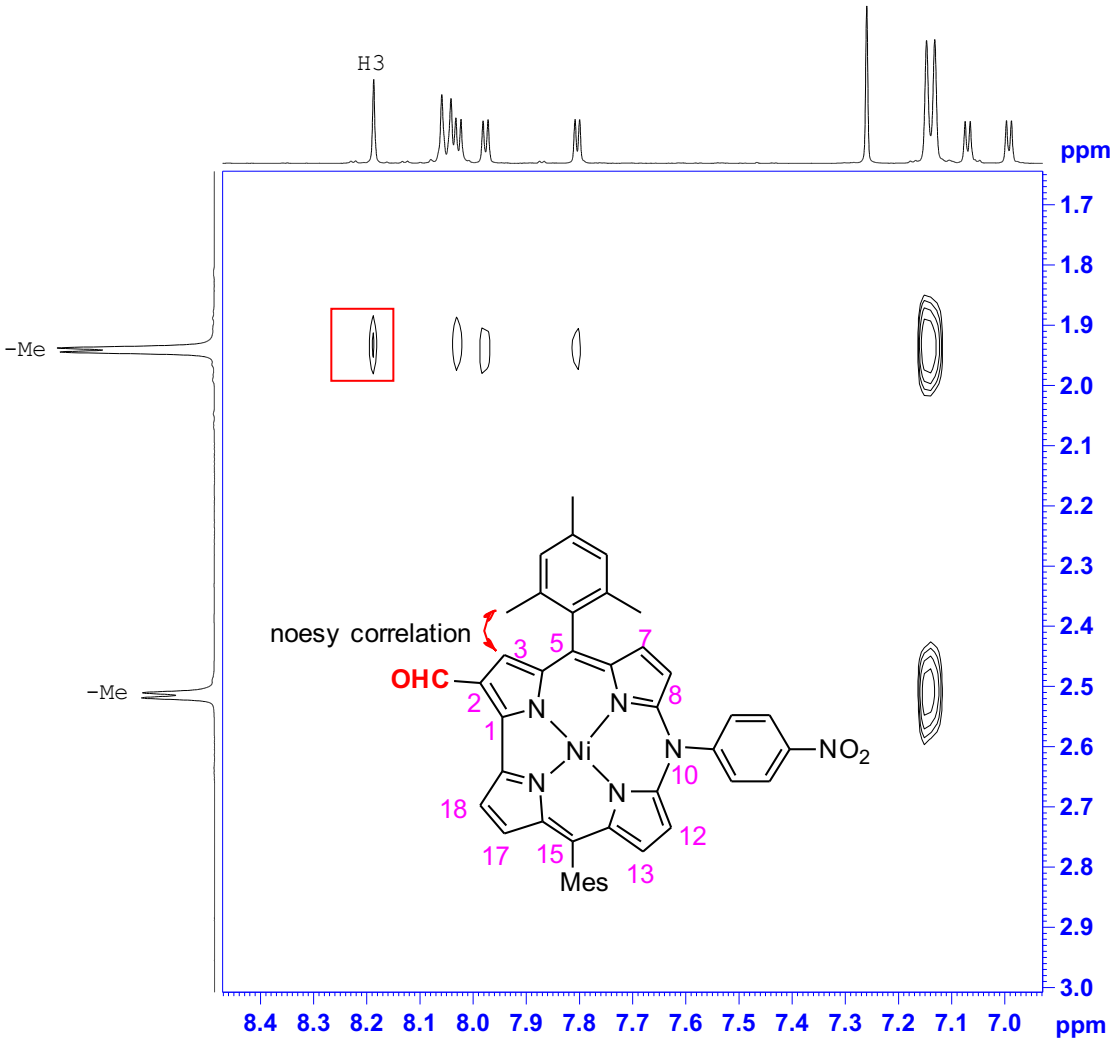

Figure S8. Magnified ^{1}H–^{1}H NOESY spectrum of **3** (500 MHz, 298 K, $CDCl_3$).

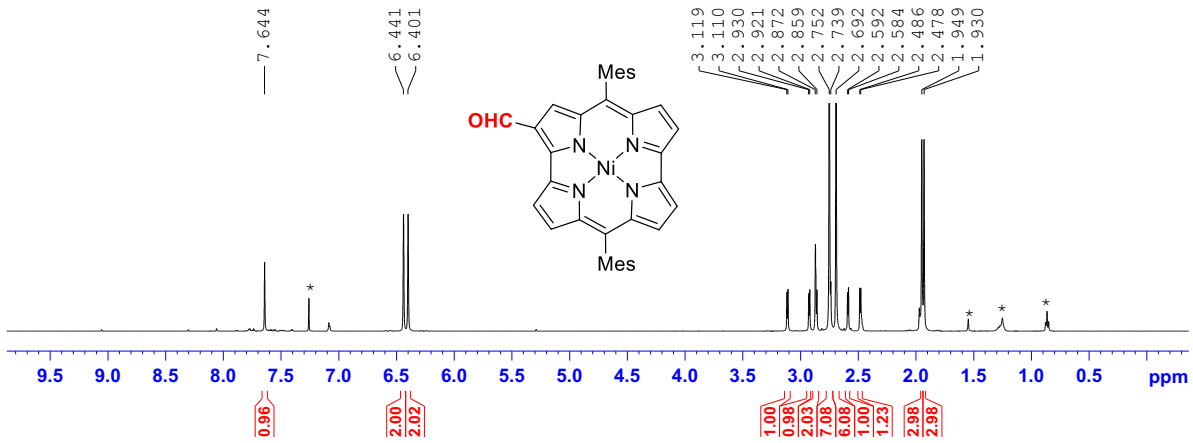

Figure S9. ^{1}H NMR spectrum of **NC-1** (500 MHz, 298 K, $CDCl_3$).

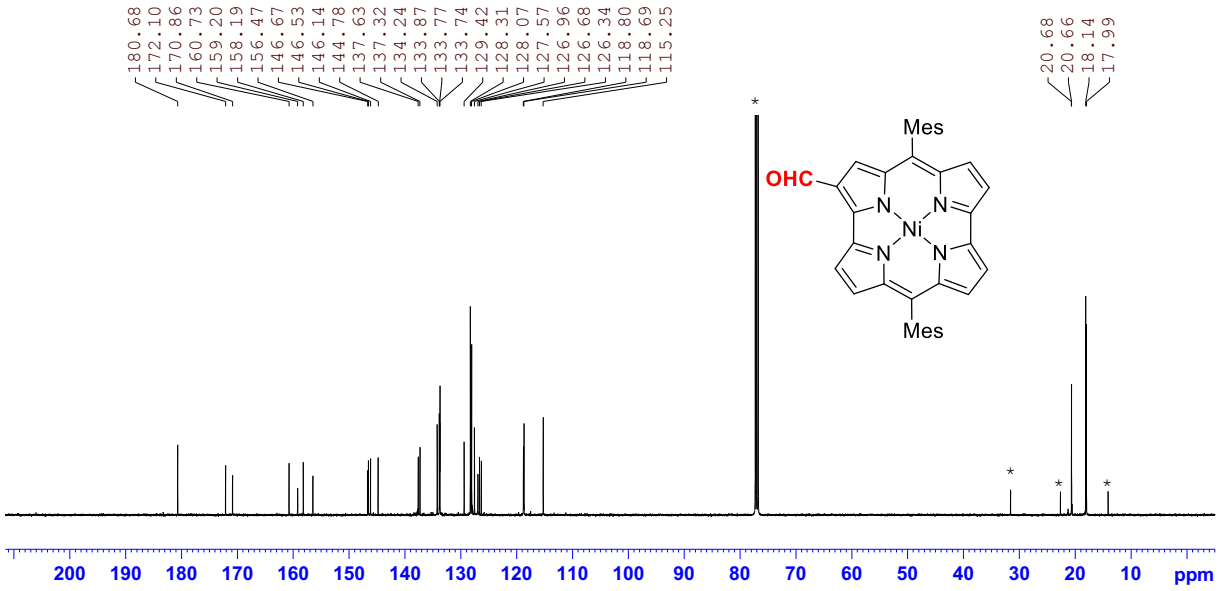

Figure S10. ^{13}C NMR spectrum of **NC-1** (125 MHz, 298 K, $CDCl_3$).

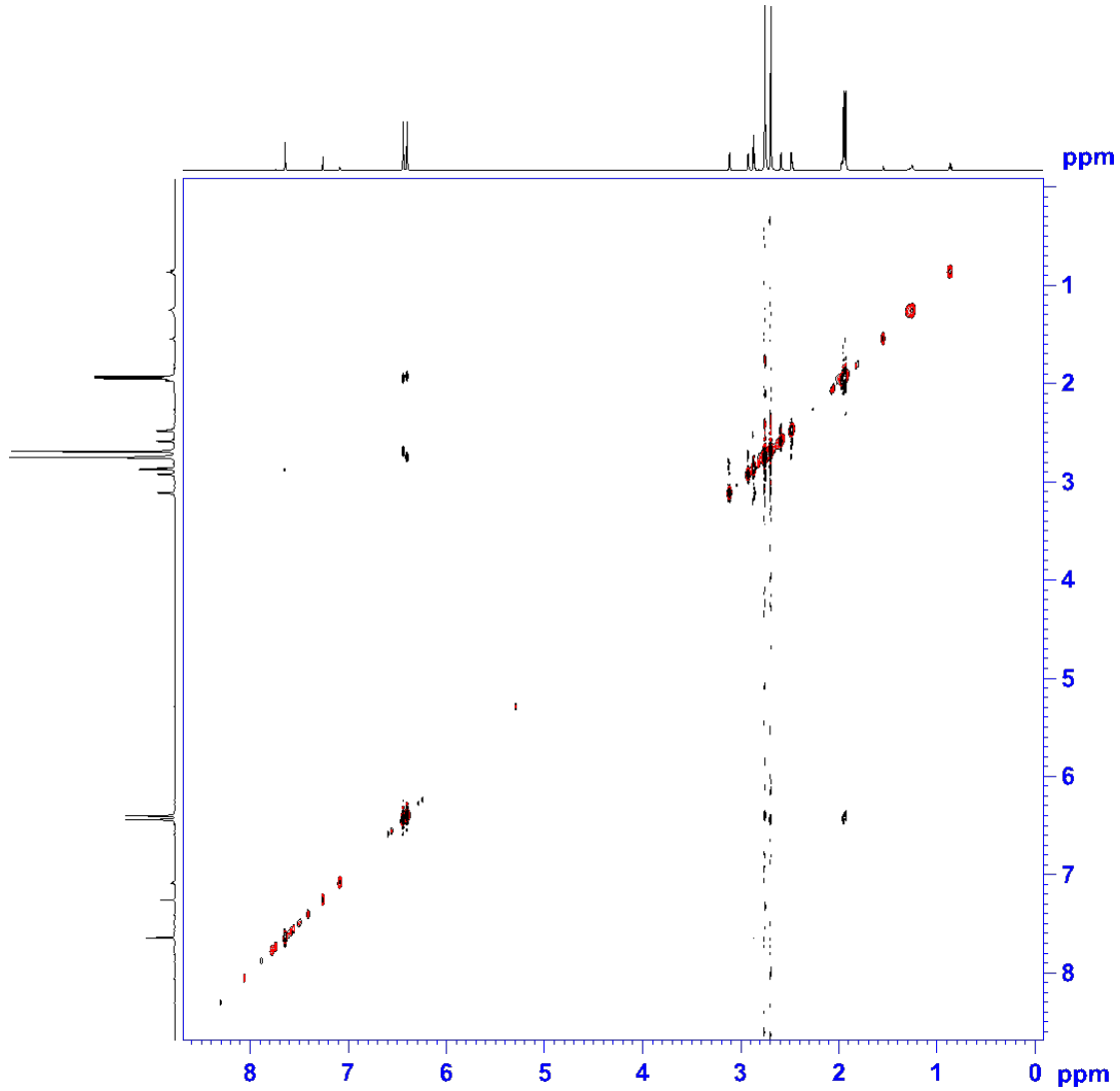

Figure S11. ^{1}H–^{1}H NOESY spectrum of **NC-1** (500 MHz, 298 K, $CDCl_3$).

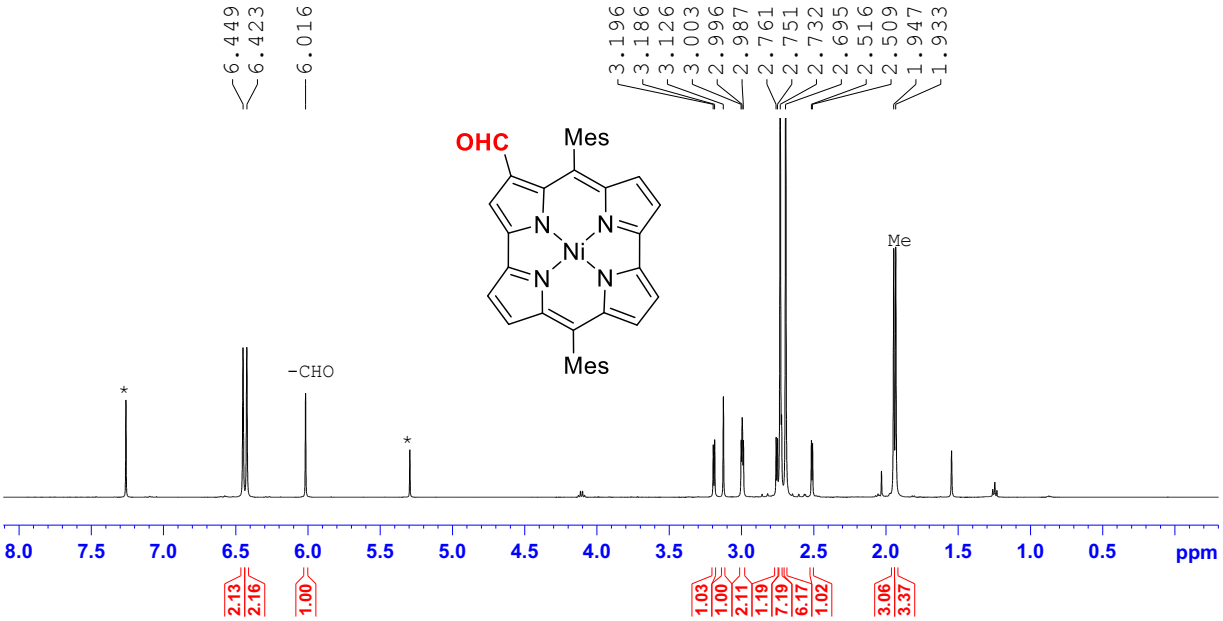

Figure S12. ^{1}H NMR spectrum of **NC-2** (500 MHz, 298 K, $CDCl_3$).

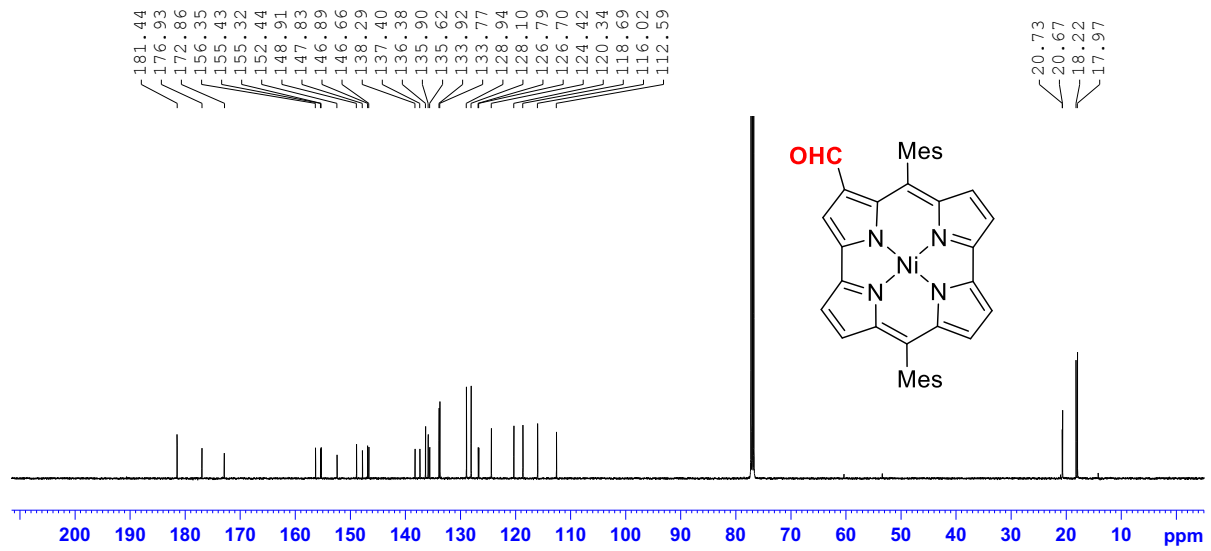

Figure S13. ^{13}C NMR spectrum of **NC-2** (125 MHz, 298 K, $CDCl_3$).

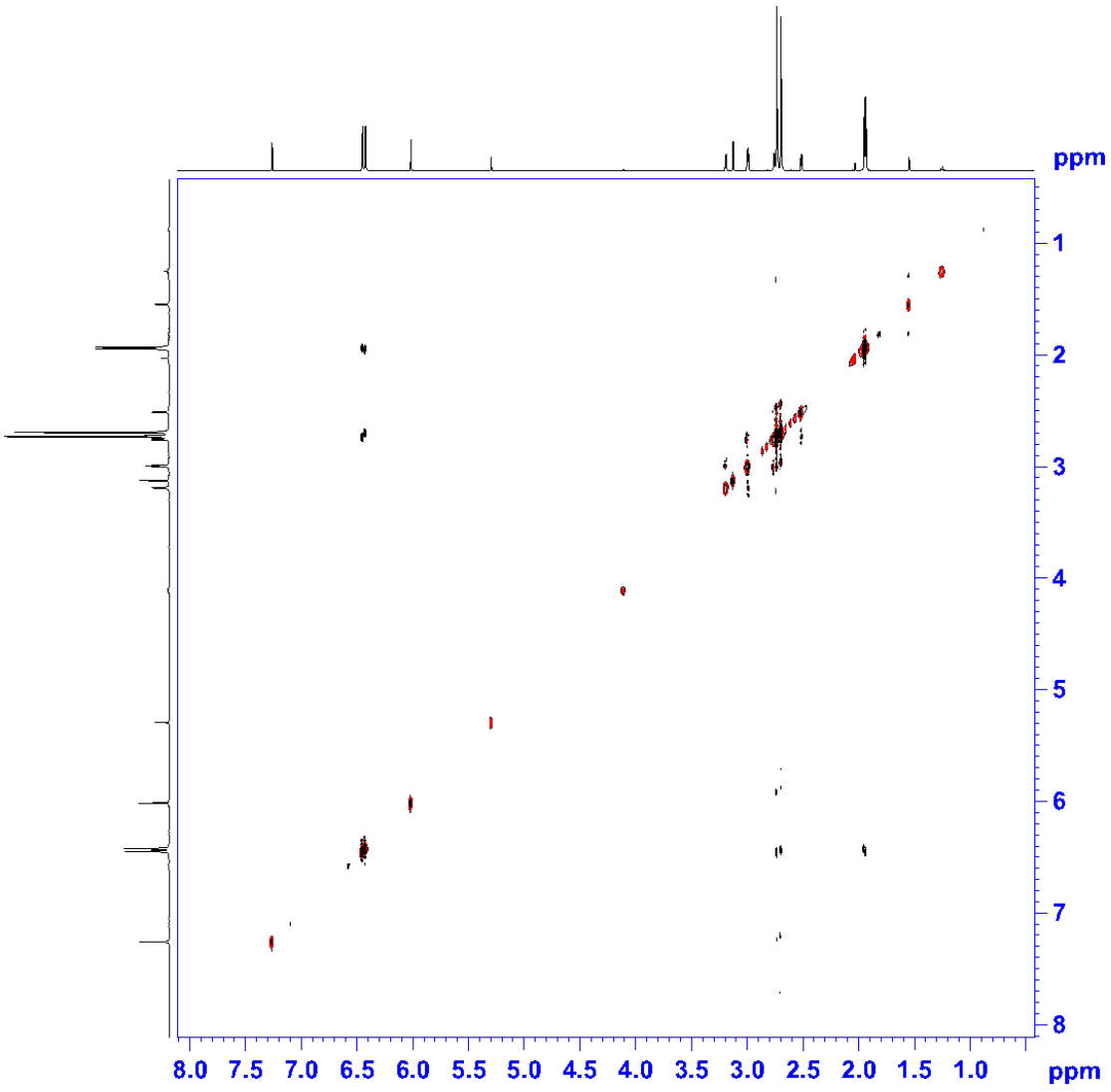

Figure S14. ^{1}H–^{1}H NOESY spectrum of **NC-2** (500 MHz, 298 K, $CDCl_3$).

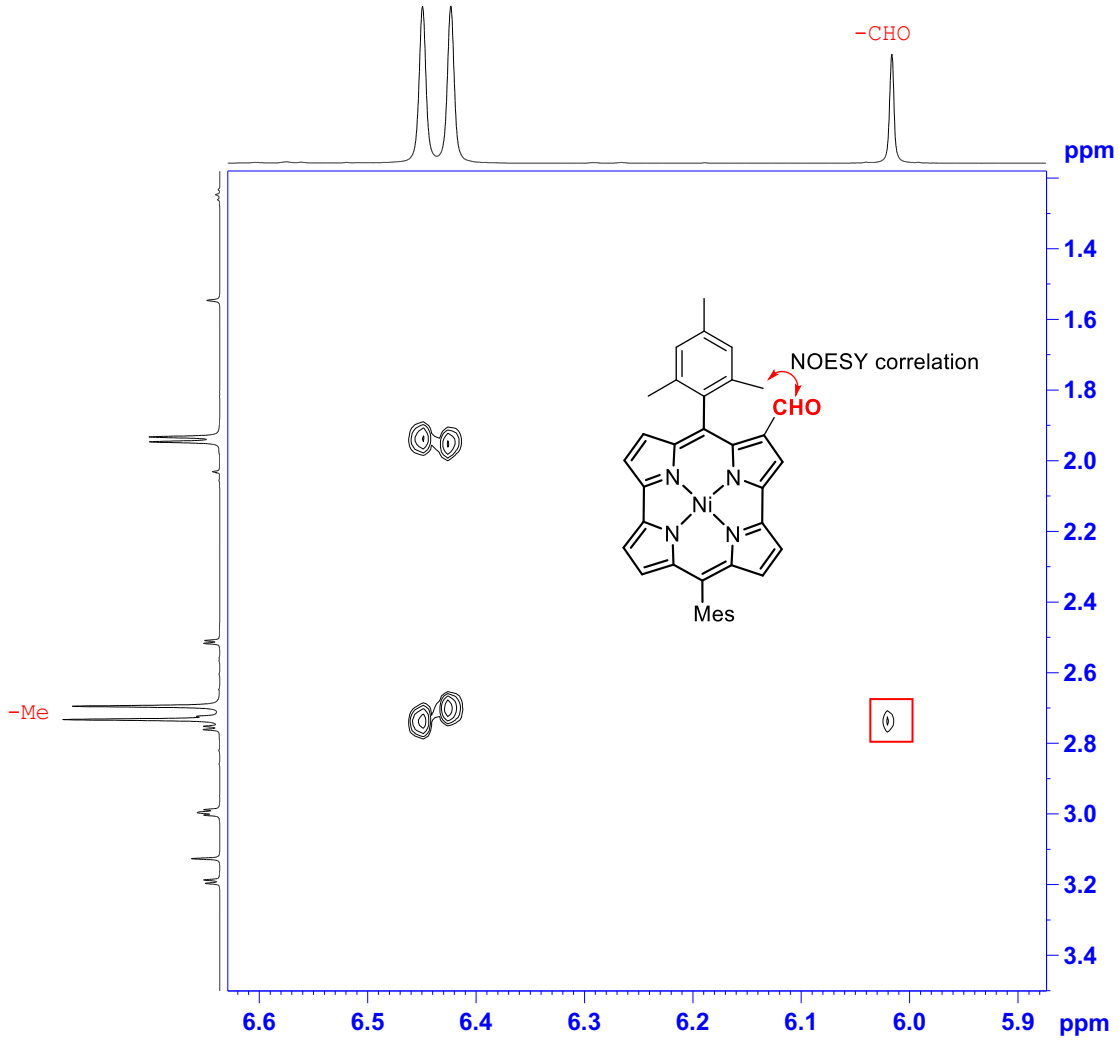

Figure S15. Magnified ^{1}H, ^{1}H NOESY spectrum of **NC-2** (500 MHz, 298 K, $CDCl_3$).

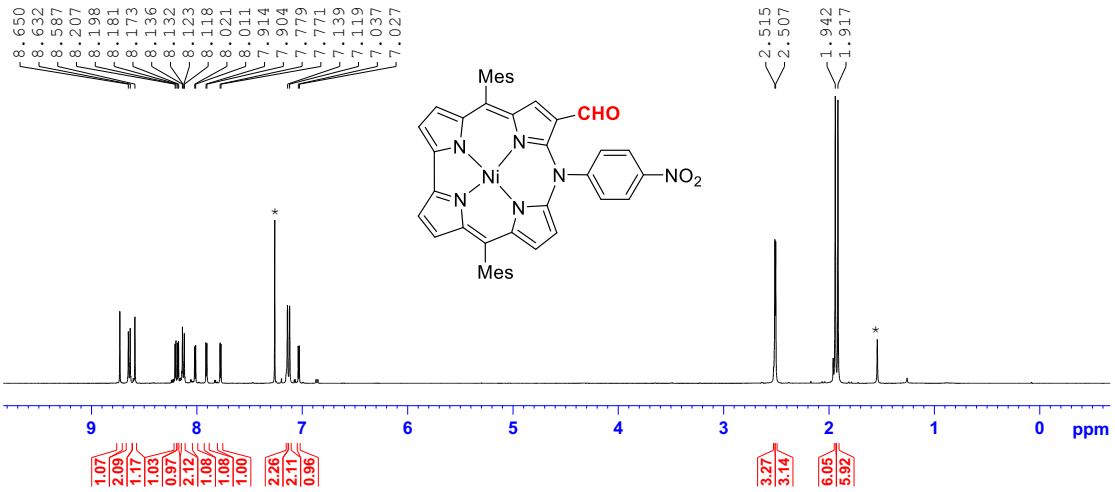

Figure S16. ^{1}H NMR spectrum of **4** (500 MHz, 298 K, $CDCl_3$).

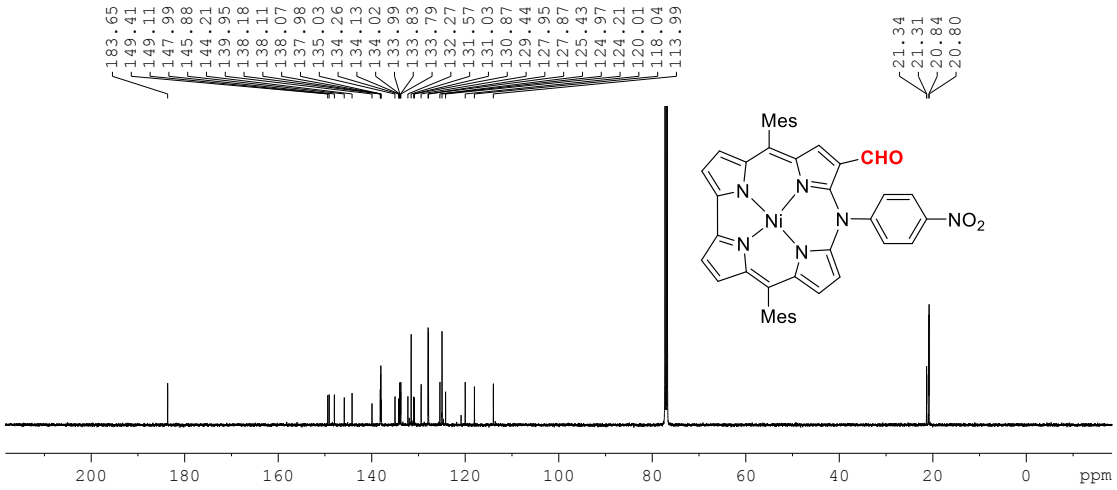

Figure S17. ^{13}C NMR spectrum of **4** (125 MHz, 298 K, $CDCl_3$).

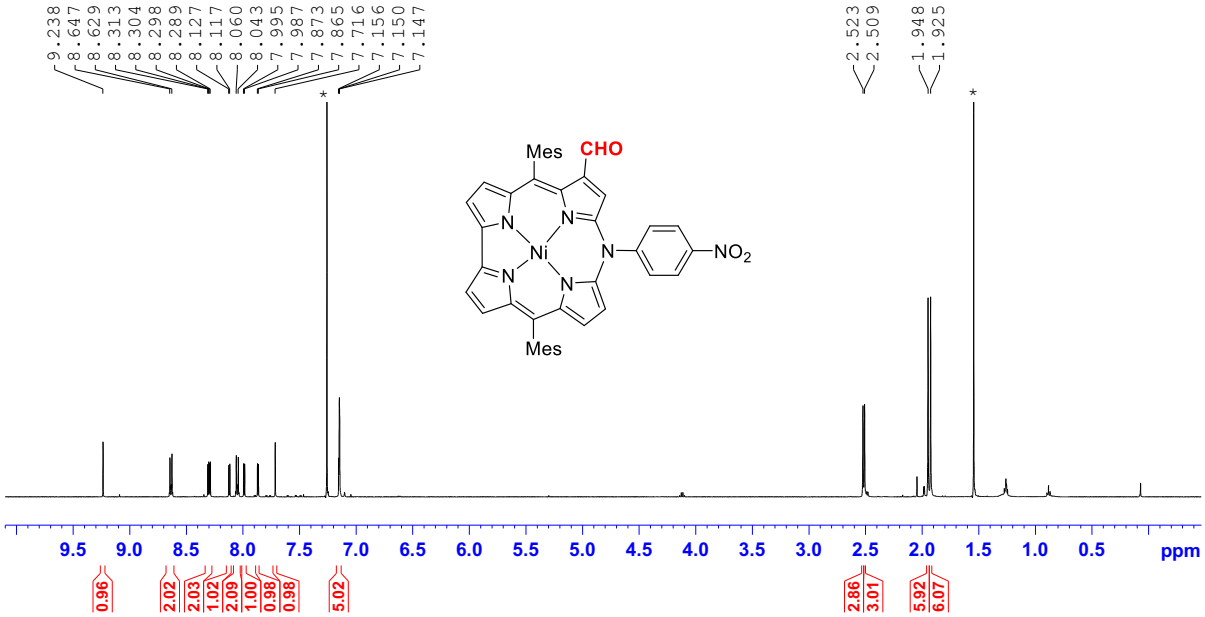

Figure S18. ^{1}H NMR spectrum of **5** (500 MHz, 298 K, $CDCl_3$).

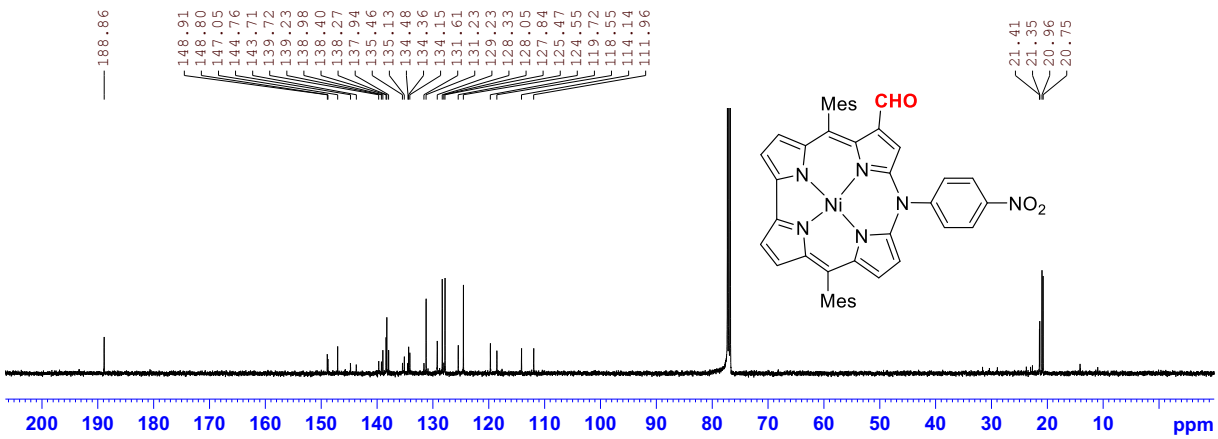

Figure S19. ^{13}C NMR spectrum of **5** (125 MHz, 298 K, $CDCl_3$).

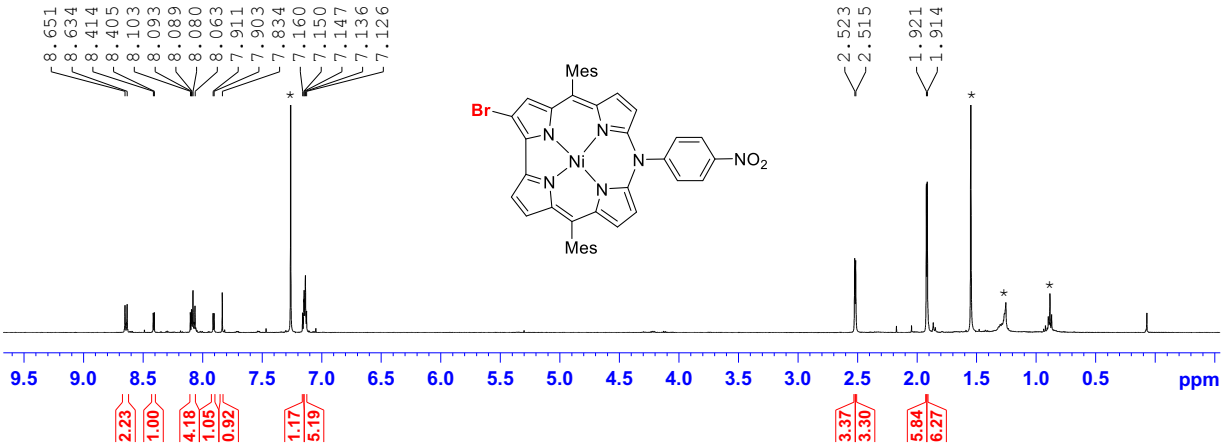

Figure S20. ^{1}H NMR spectrum of **6** (500 MHz, 298 K, $CDCl_3$).

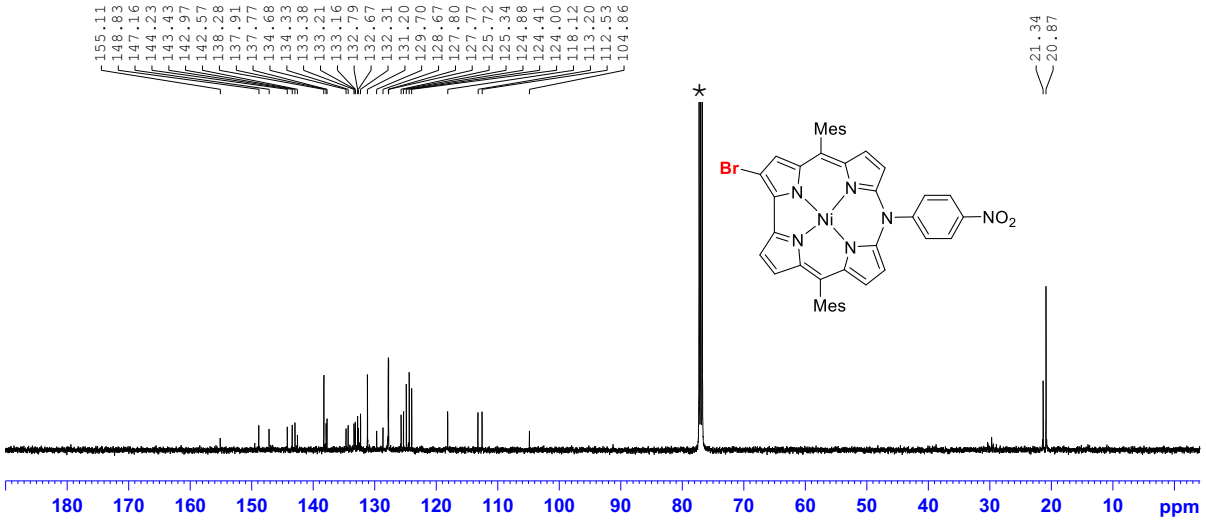

Figure S21. ^{13}C NMR spectrum of **6** (125 MHz, 298 K, $CDCl_3$).

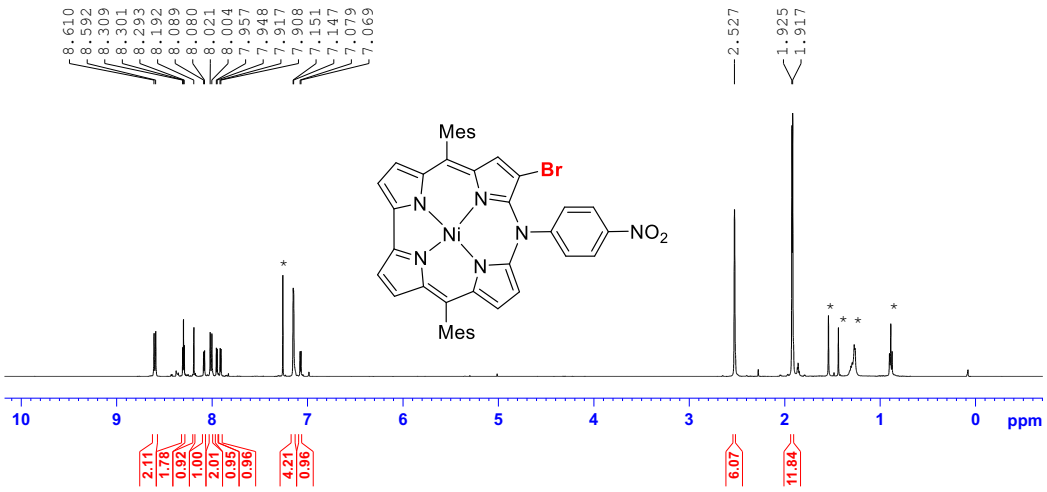

Figure S22. ^{1}H NMR spectrum of **7** (500 MHz, 298 K, $CDCl_3$).

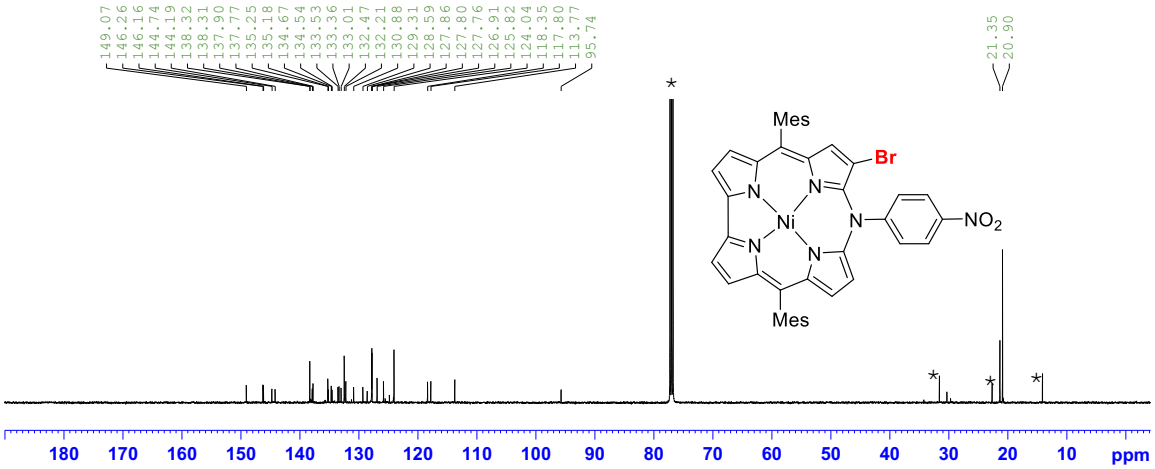

Figure S23. ^{13}C NMR spectrum of **7** (125 MHz, 298 K, $CDCl_3$).

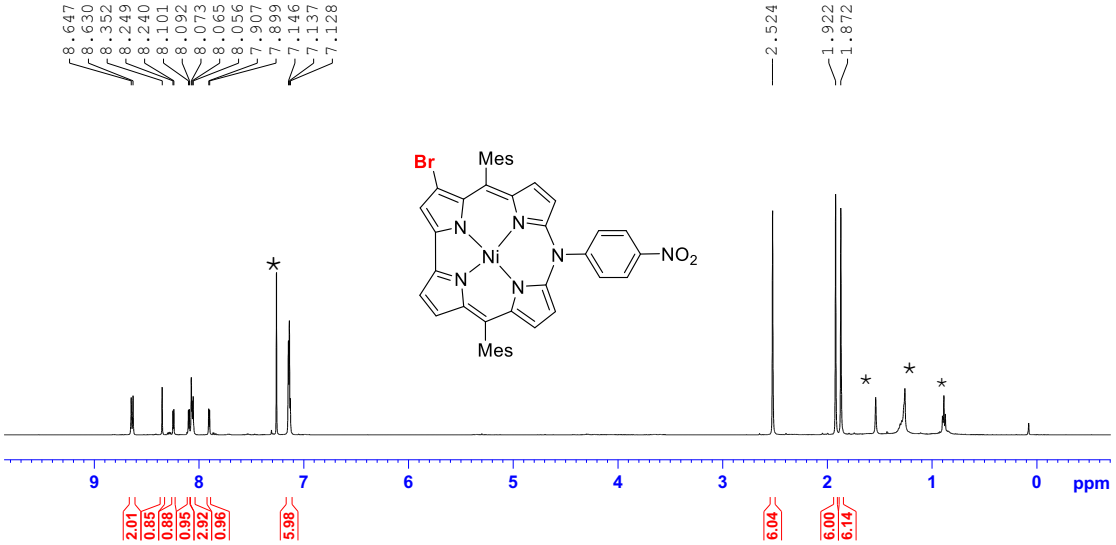

Figure S24. ^{1}H NMR spectrum of **8** (500MHz, 298 K, $CDCl_3$).

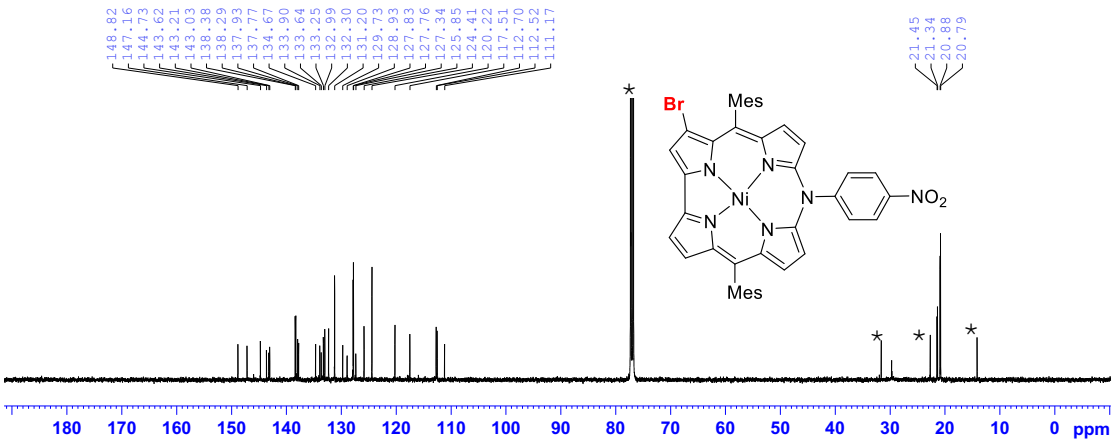

Figure S25. ^{13}C NMR spectrum of **8** (125 MHz, 298 K, $CDCl_3$).

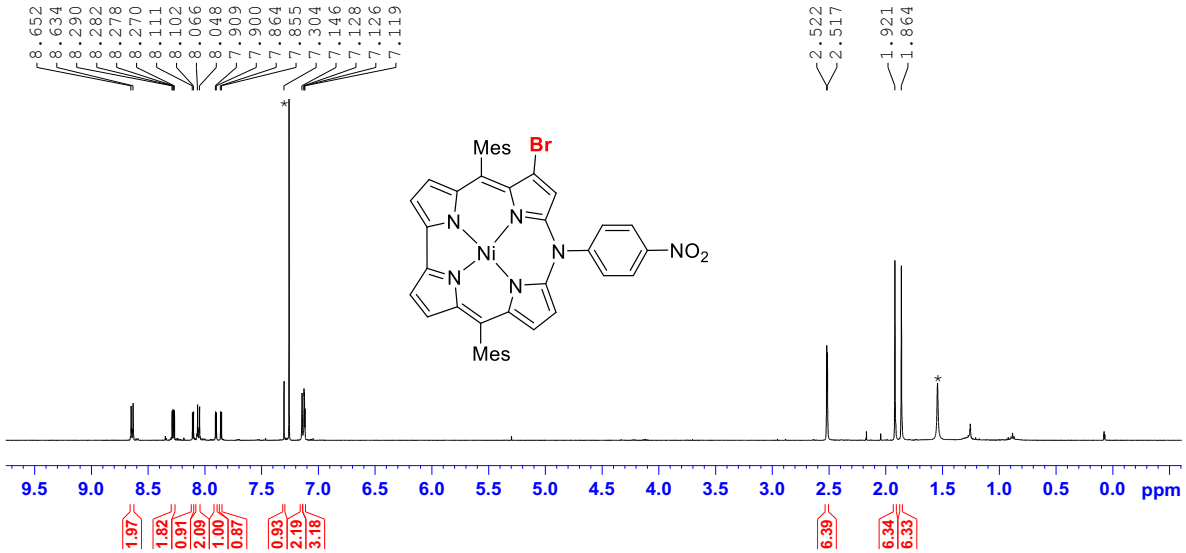

Figure S26. ^{1}H NMR spectrum of **9** (500MHz, 298 K, $CDCl_3$).

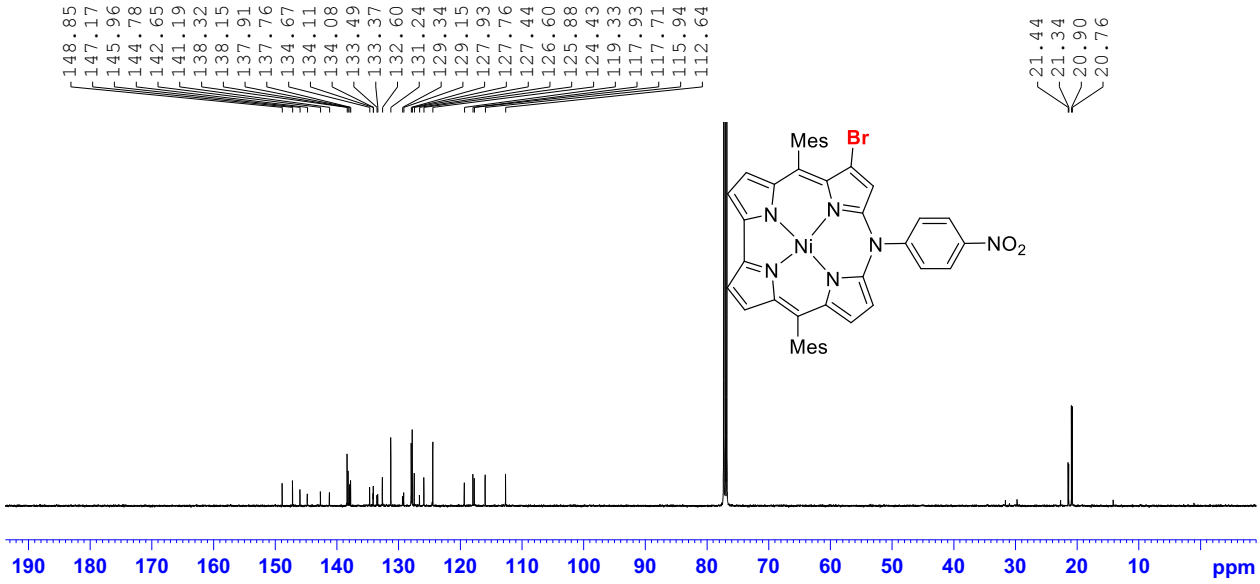

Figure S27. ^{13}C NMR spectrum of **9** (125 MHz, 298 K, $CDCl_3$).

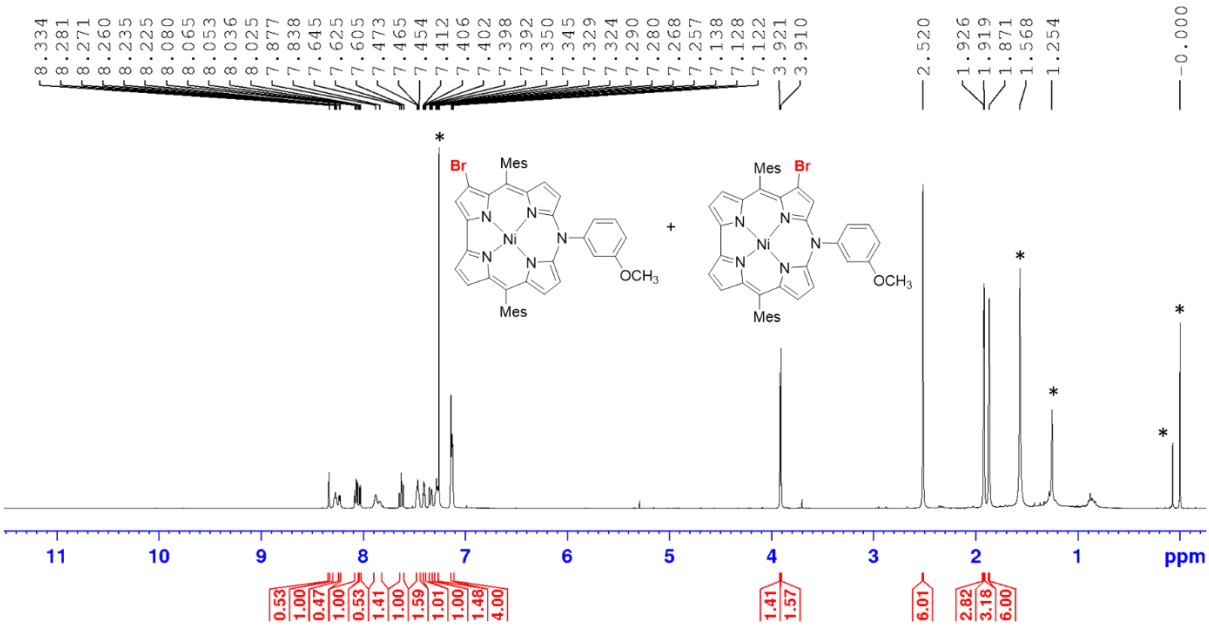

Figure S28. ^{1}H NMR spectrum of a mixture of **10** and **11** (400 MHz, 298 K, $CDCl_3$).

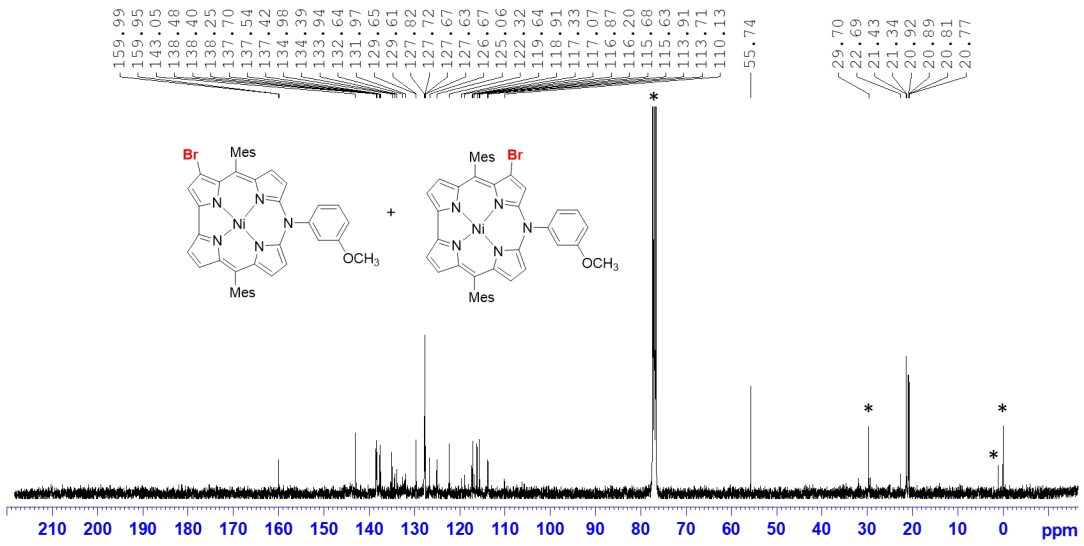

Figure S29. ^{13}C NMR spectrum of a mixture of **10** and **11** (100 MHz, 298 K, $CDCl_3$).

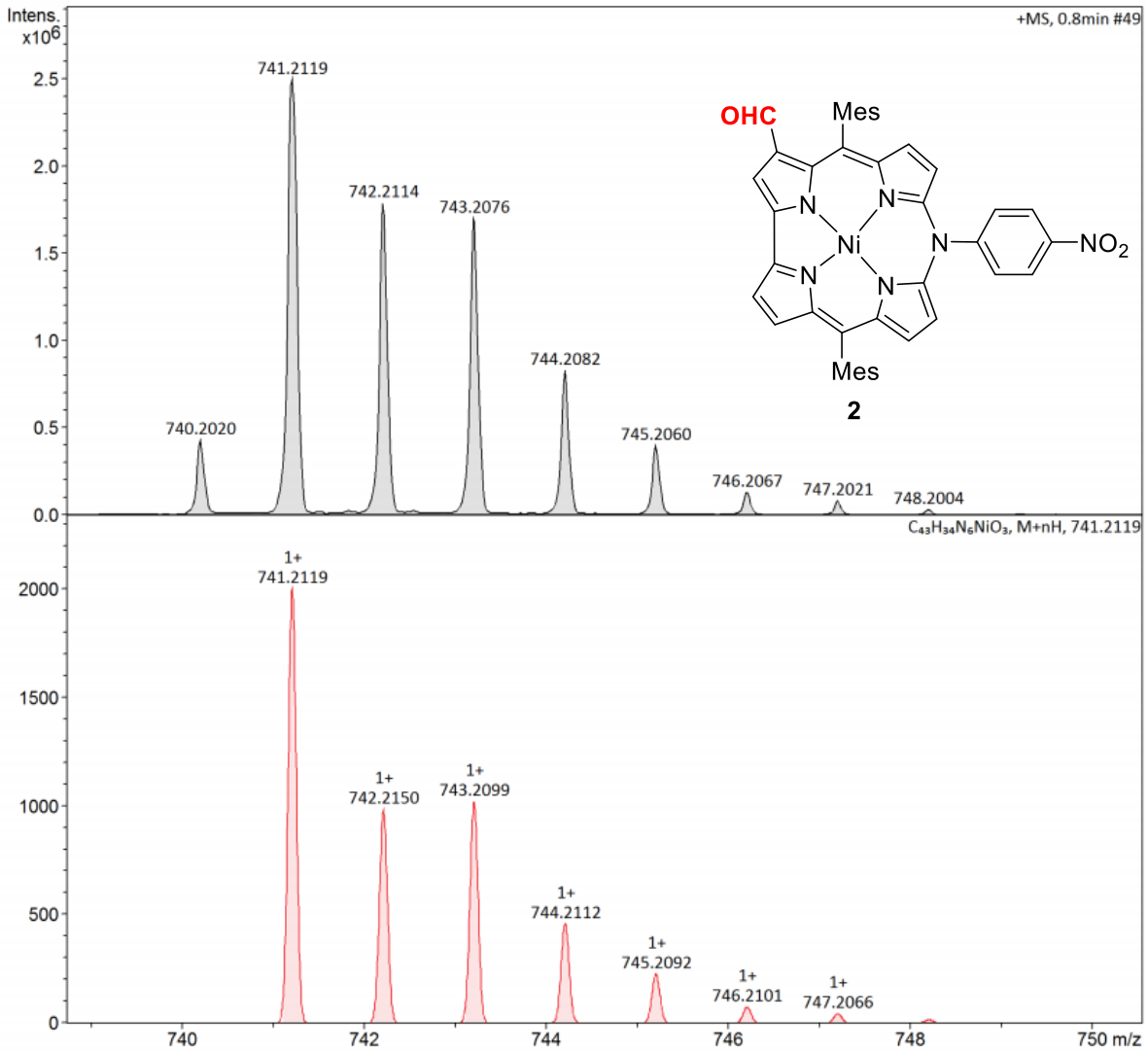

Figure S30. HR-APCI-TOF-MS spectrum of **2** (experimental: upper trace; simulated: red bottom trace).

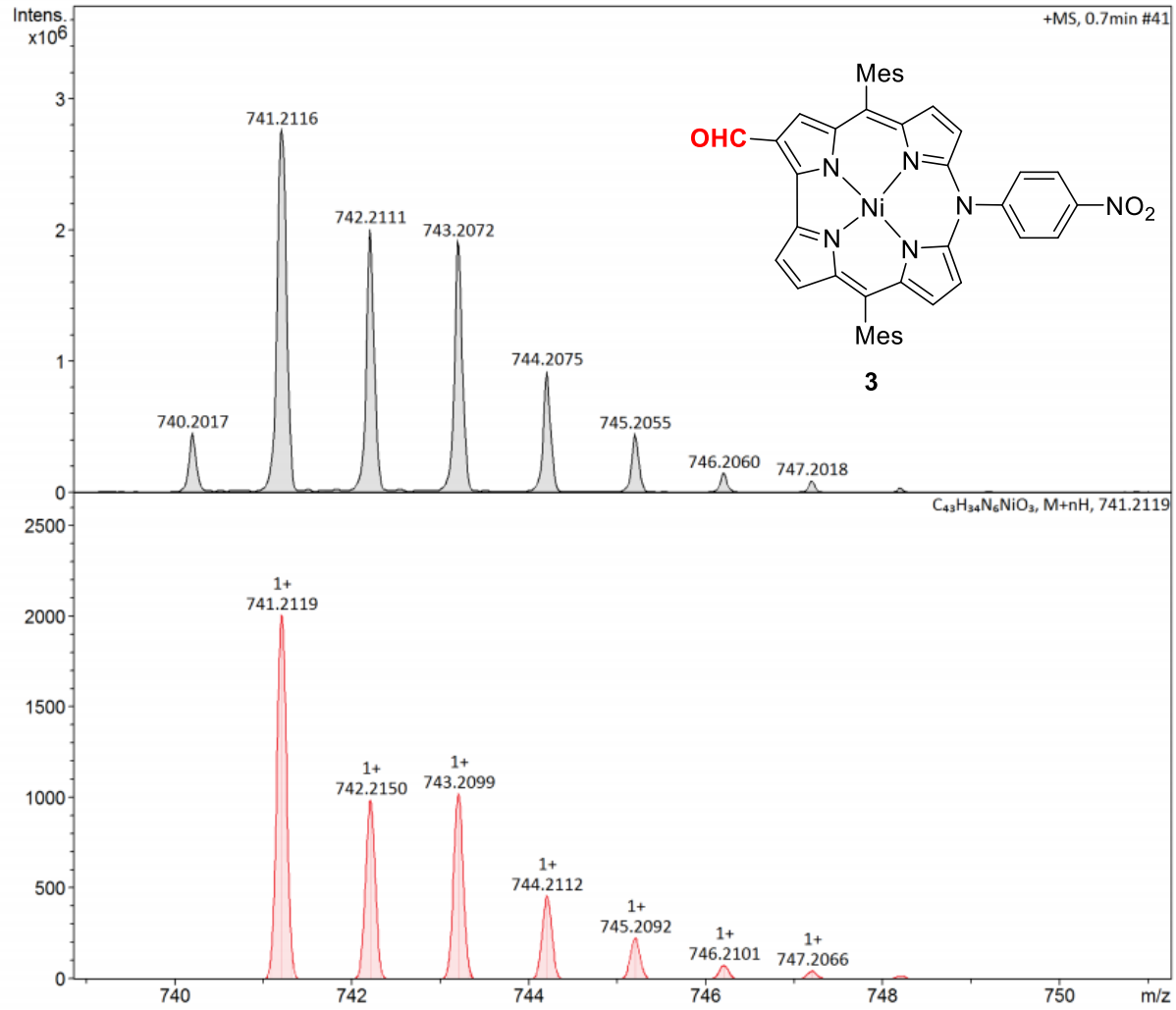

Figure S31. HR-APCI-TOF-MS spectrum of **3** (experimental: upper trace; simulated: red bottom trace).

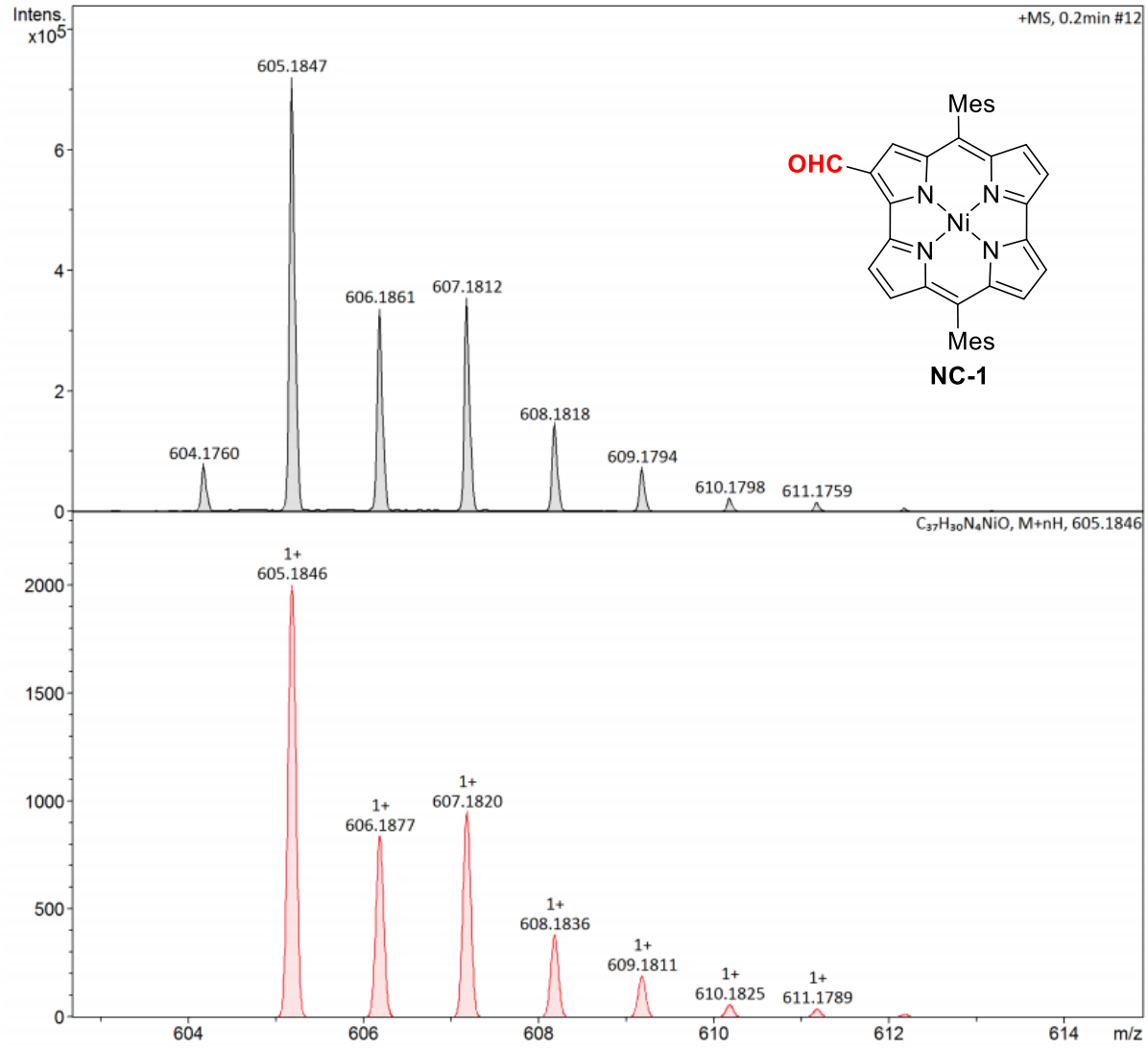

Figure S32. HR-APCI-TOF-MS spectrum of **NC-1** (experimental: upper trace; simulated: red bottom trace).

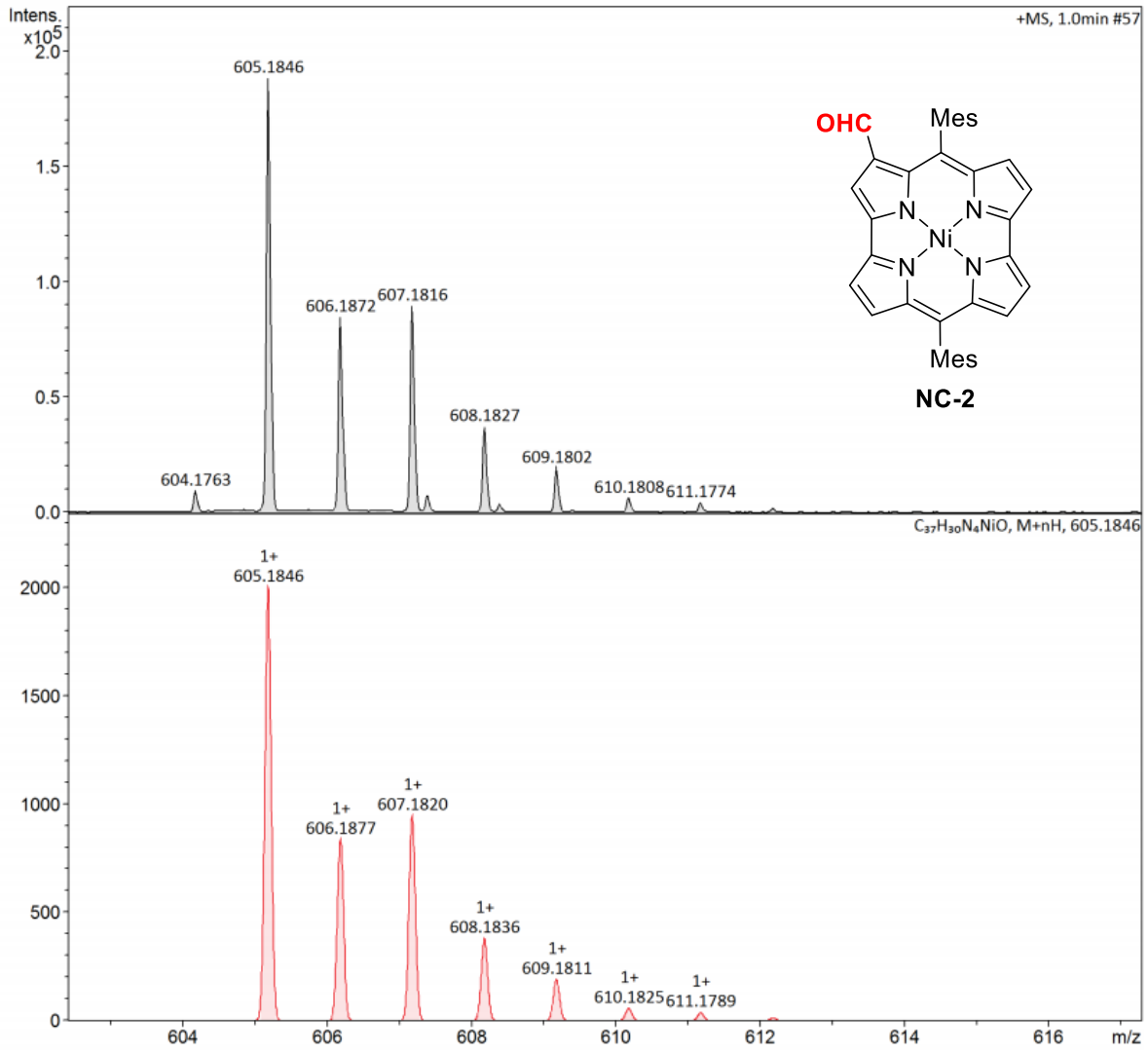

Figure S33. HR-APCI-TOF-MS spectrum of **NC-2** (experimental: upper trace; simulated: red bottom trace).

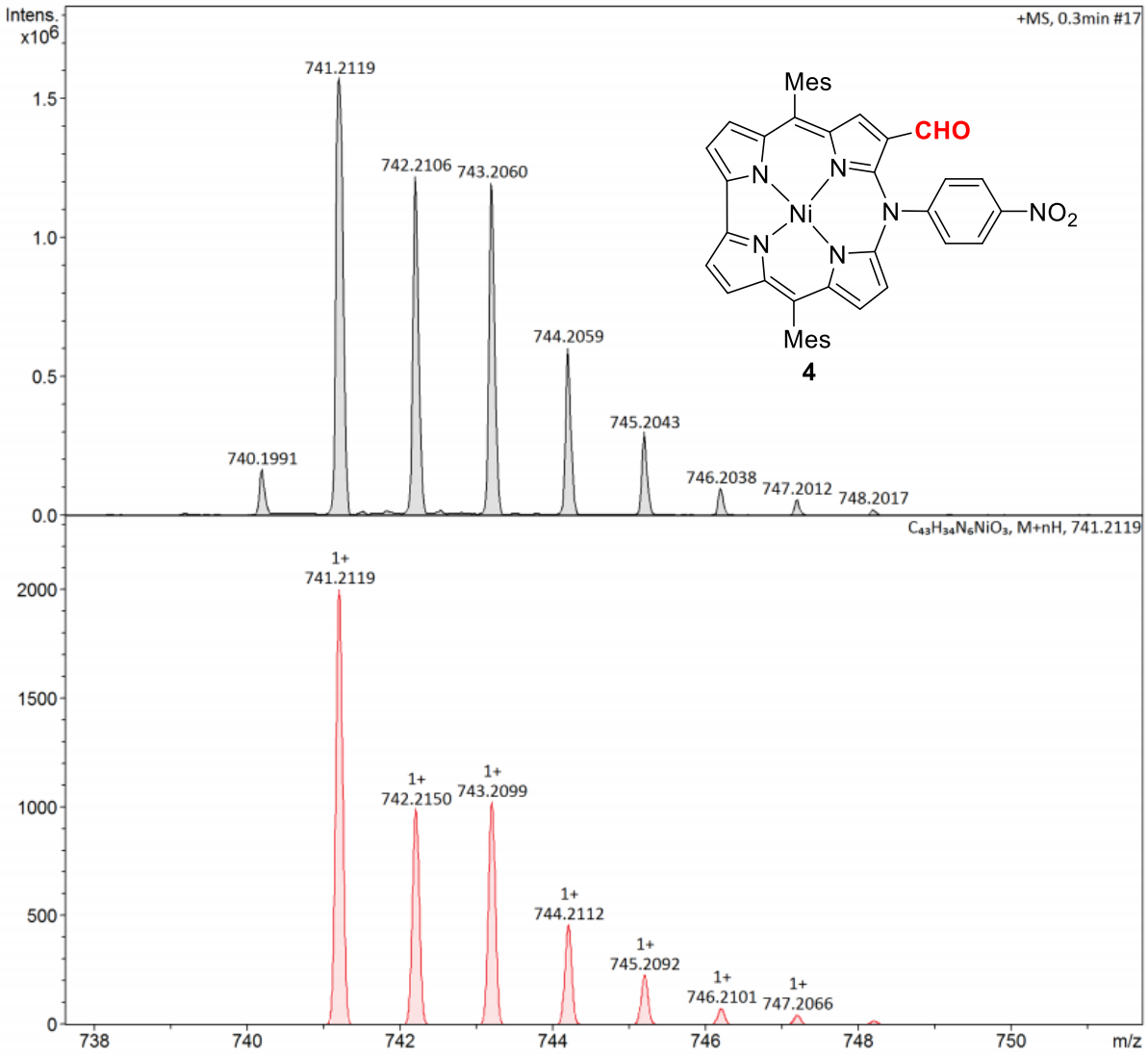

Figure S34. HR-APCI-TOF-MS spectrum of **4** (experimental: upper trace; simulated: red bottom trace).

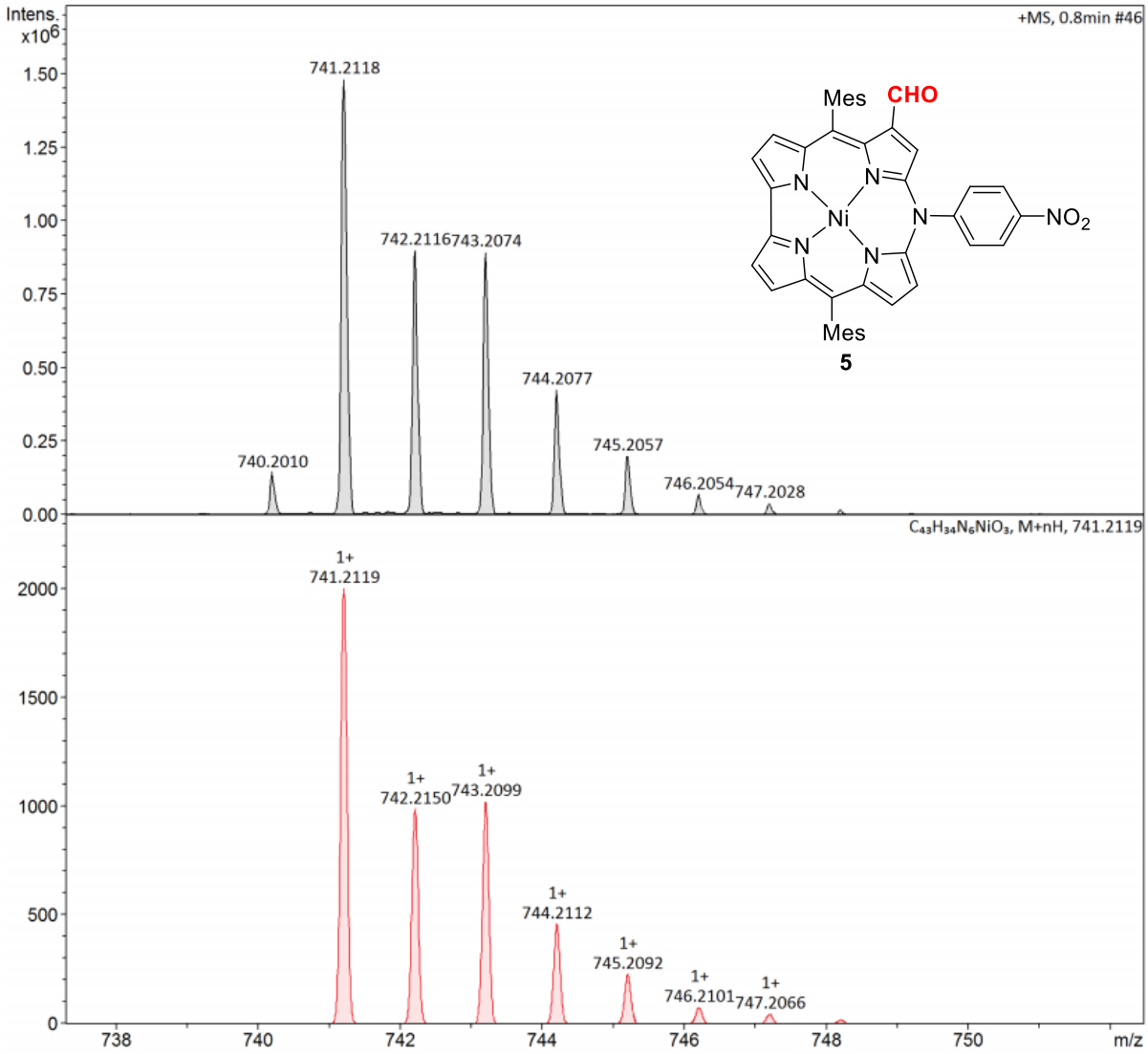

Figure S35. HR-APCI-TOF-MS spectrum of **5** (experimental: upper trace; simulated: red bottom trace).

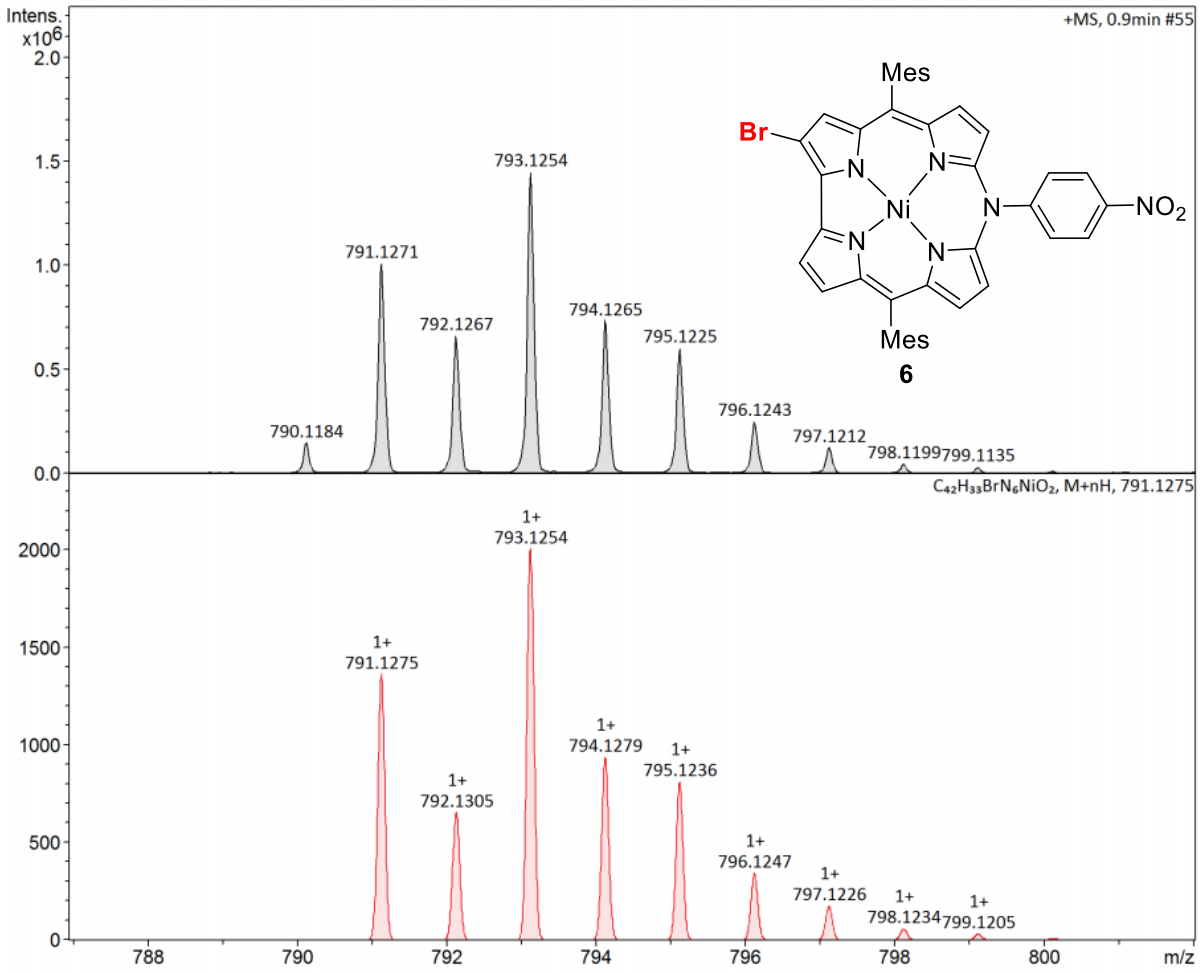

Figure S36. HR-APCI-TOF-MS spectrum of **6** (experimental: upper trace; simulated: red bottom trace).

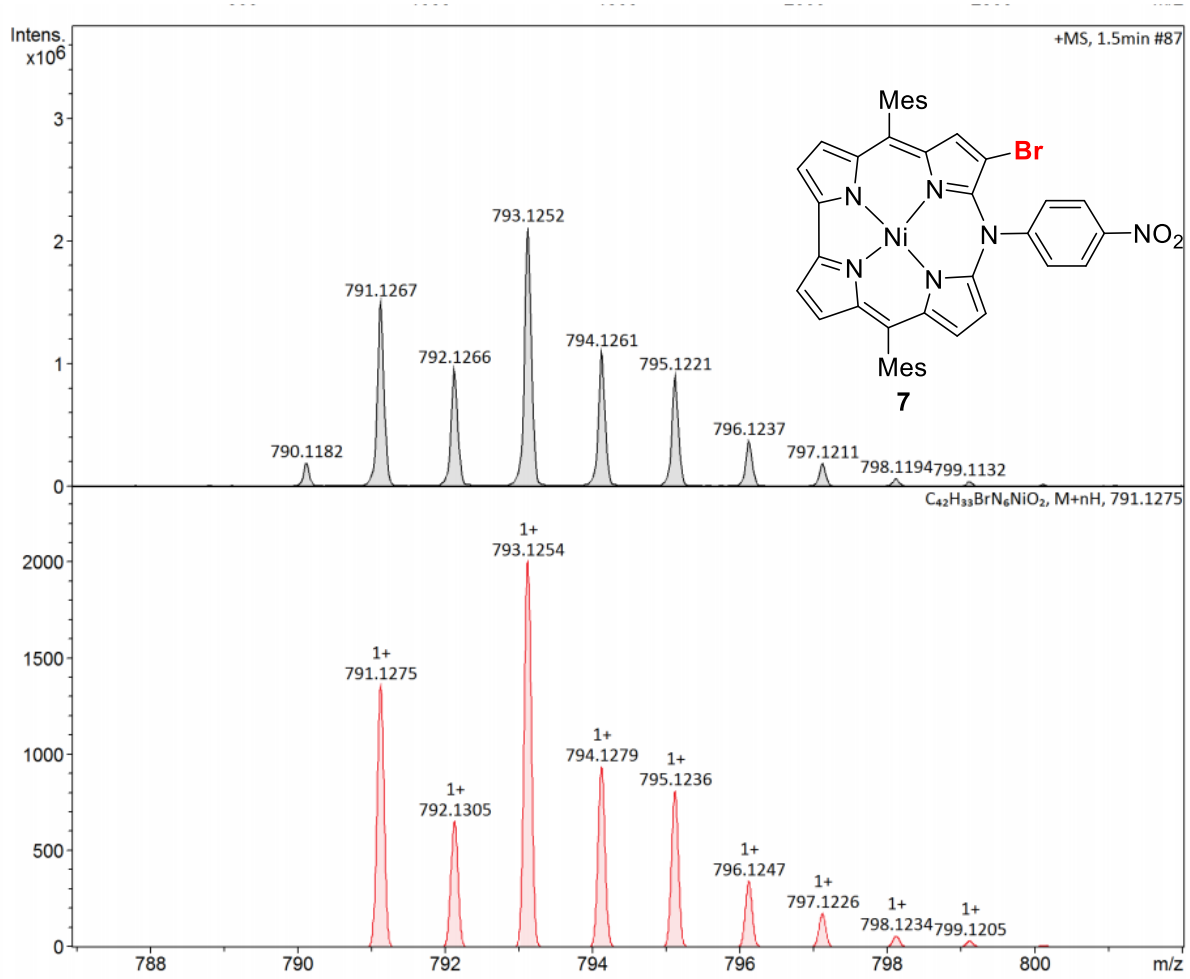

Figure S37. HR-APCI-TOF-MS spectrum of **7** (experimental: upper trace; simulated: red bottom trace).

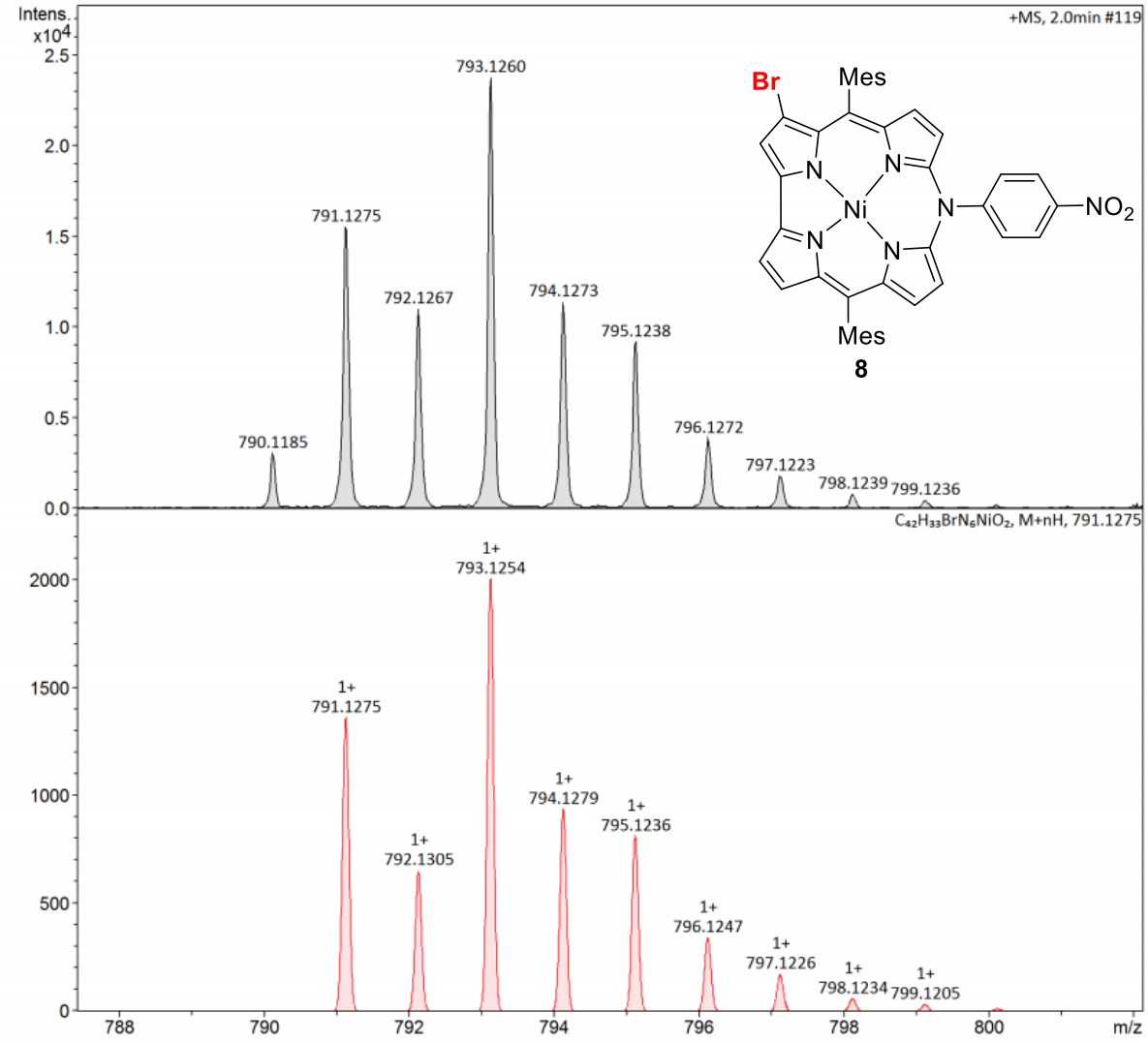

Figure S38. HR-APCI-TOF-MS spectrum of **8** (experimental: upper trace; simulated: red bottom trace).

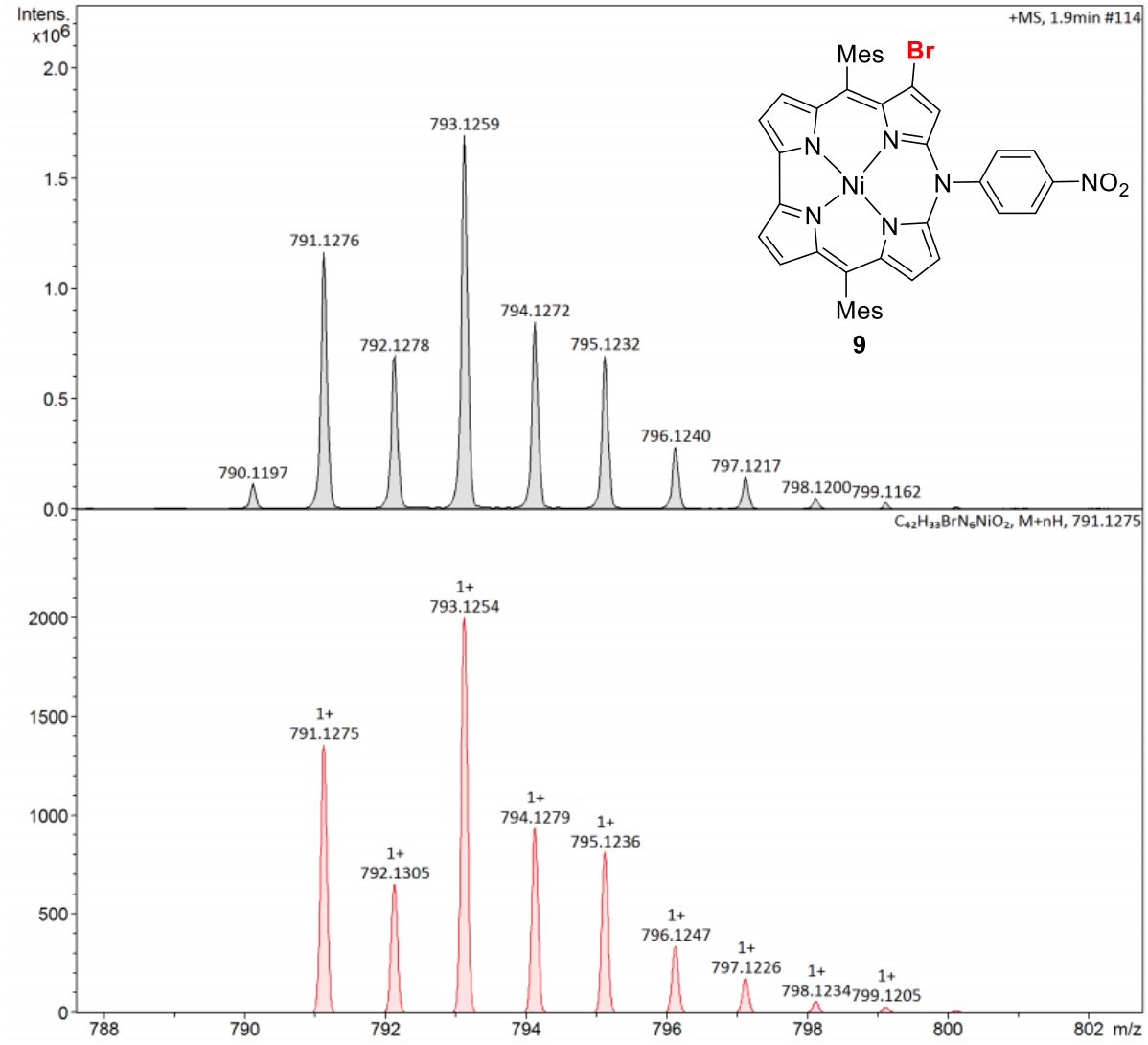

Figure S39. HR-APCI-TOF-MS spectrum of **9** (experimental: upper trace; simulated: red bottom trace).

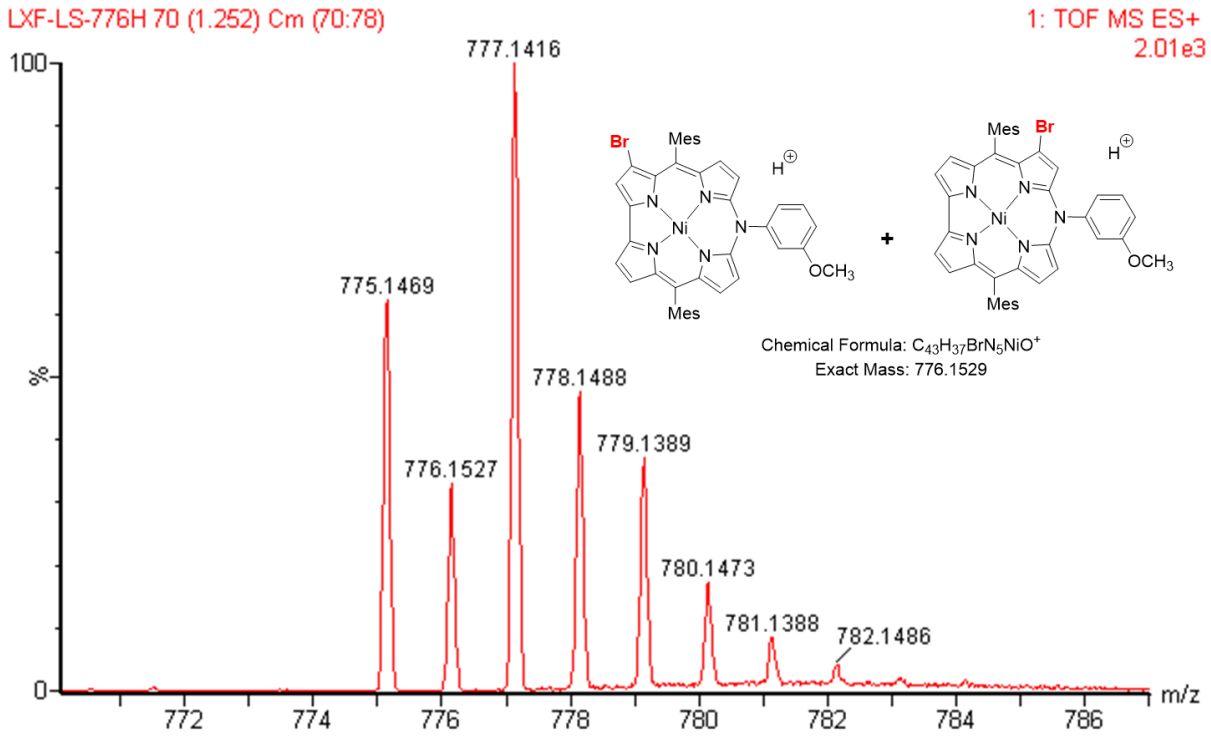

Figure S40. HR-ESI-MS spectrum of a mixture of **10** and **11**.

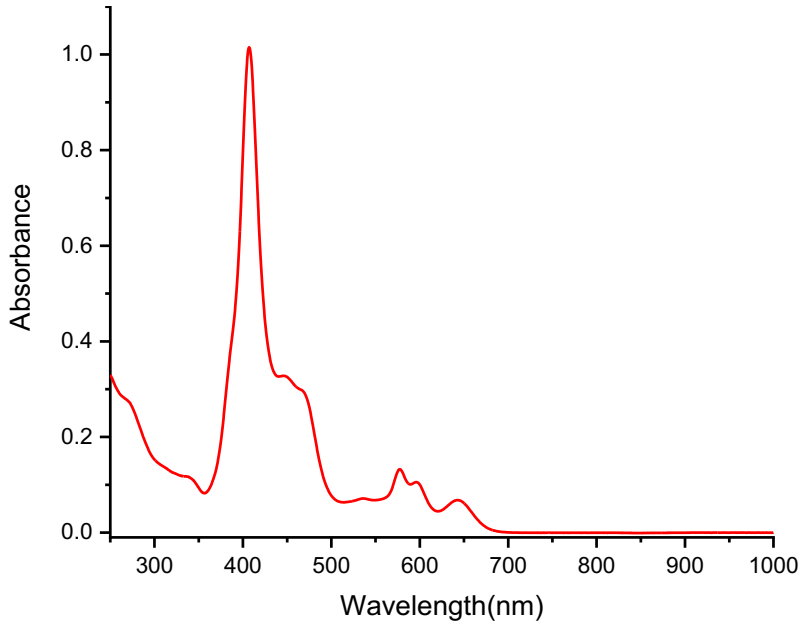

Figure S41. UV-vis absorption spectrum of **2** in CH_2Cl_2.

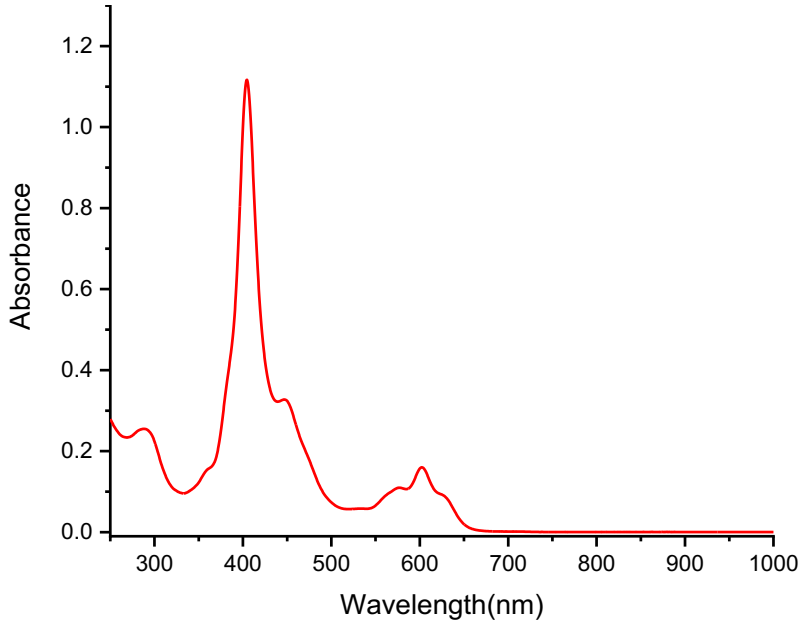

Figure S42. UV-vis absorption spectrum of **3** in CH_2Cl_2.

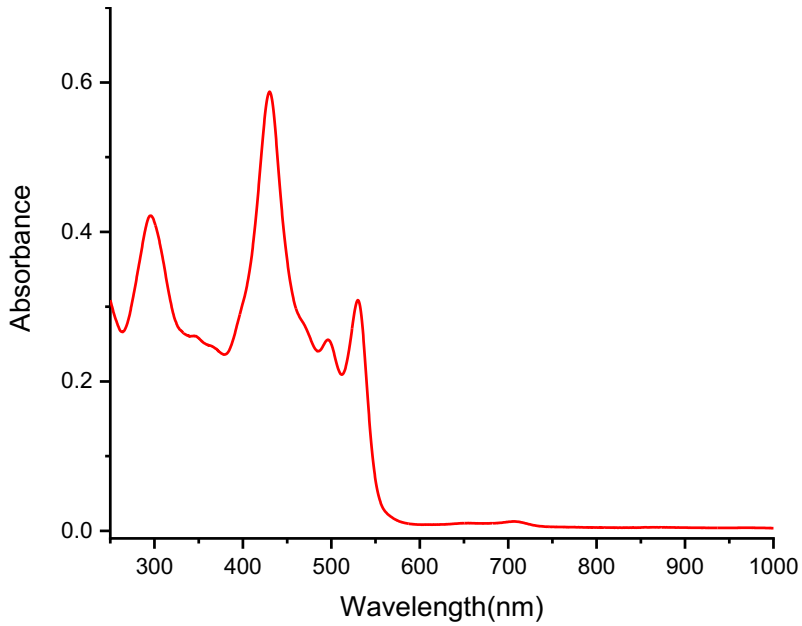

Figure S43. UV-vis absorption spectrum of **NC-1** in CH_2Cl_2.

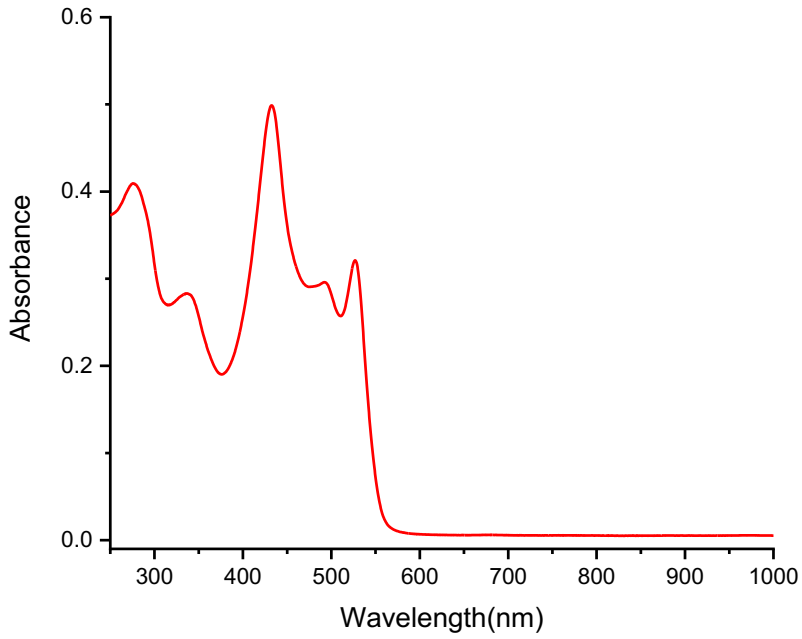

Figure S44. UV-vis absorption spectrum of **NC-2** in CH_2Cl_2.

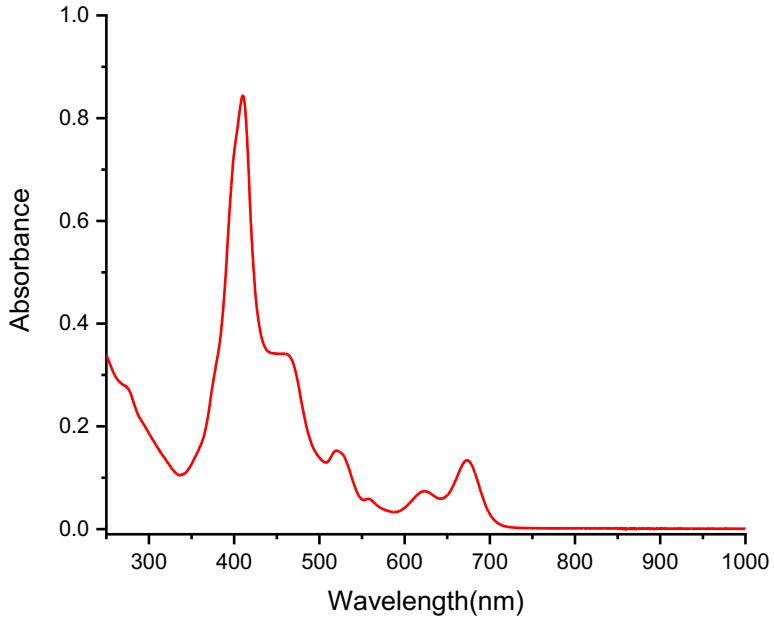

Figure S45. UV-vis absorption spectrum of **4** in CH_2Cl_2.

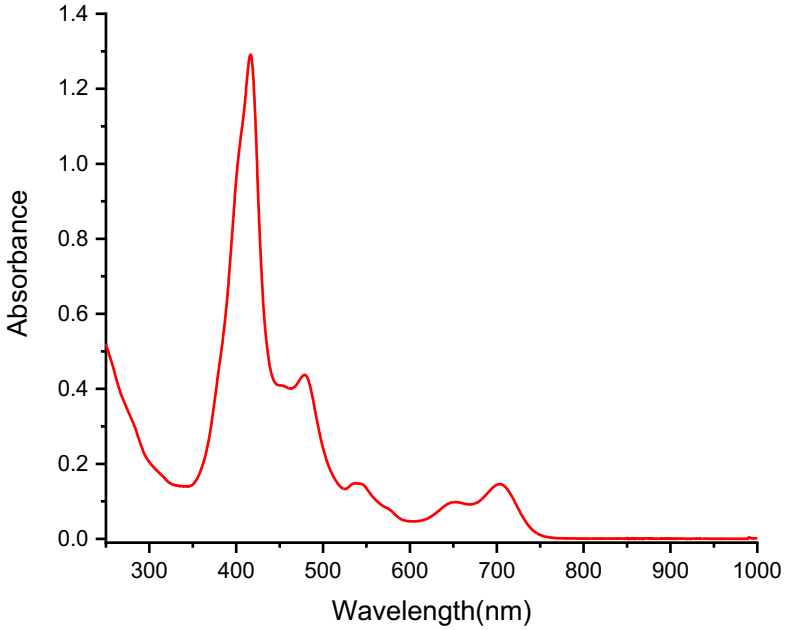

Figure S46. UV-vis absorption spectrum of **5** in CH_2Cl_2.

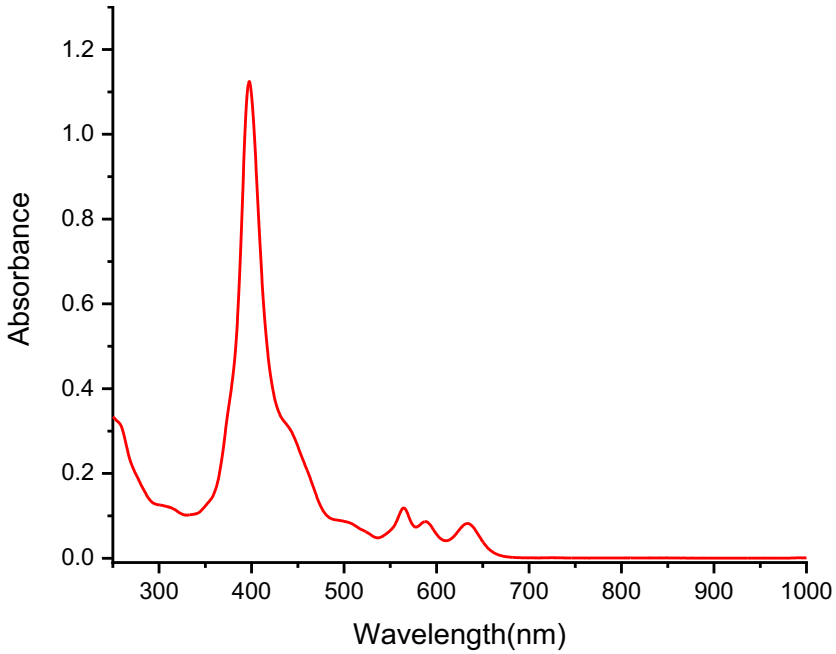

Figure S47. UV-vis absorption spectrum of **6** in CH_2Cl_2.

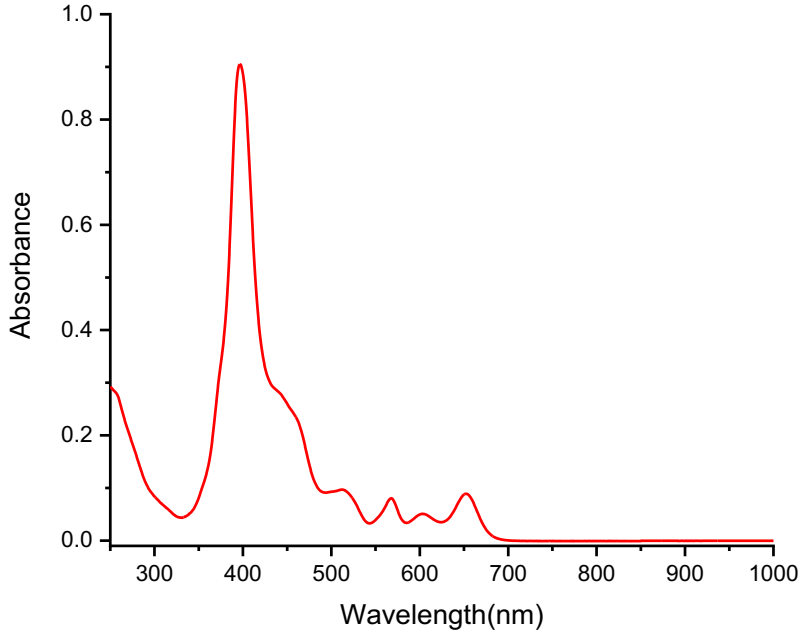

Figure S48. UV-vis absorption spectrum of **7** in CH_2Cl_2.

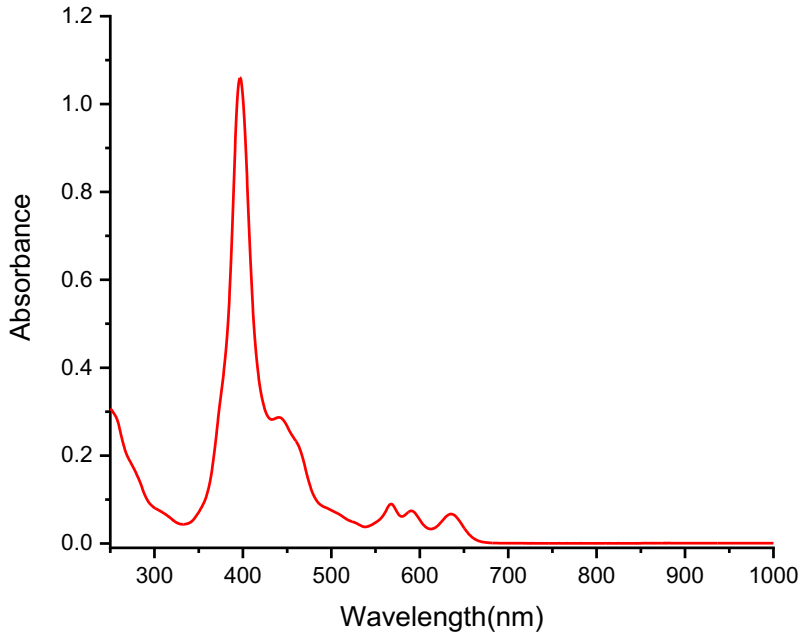

Figure S49. UV-vis absorption spectrum of **8** in CH_2Cl_2.

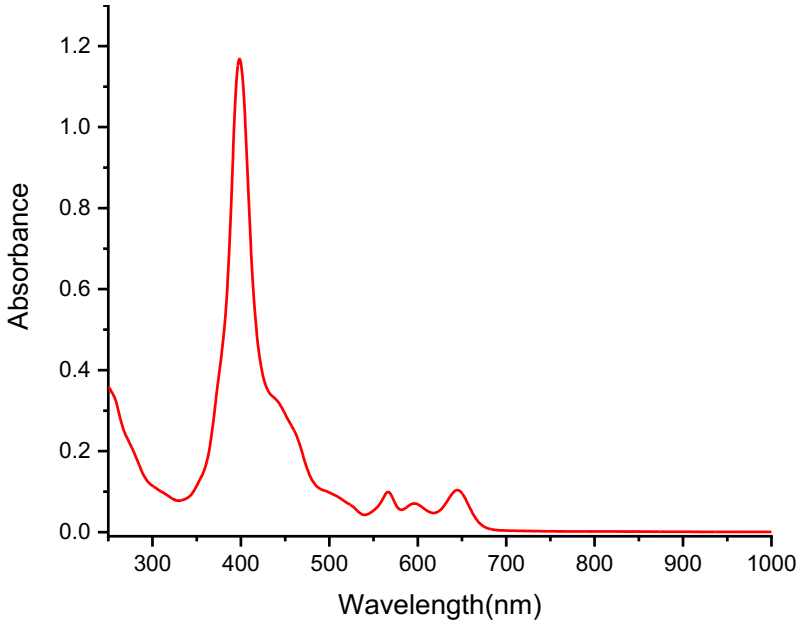

Figure S50. UV-vis absorption spectrum of **9** in CH_2Cl_2.

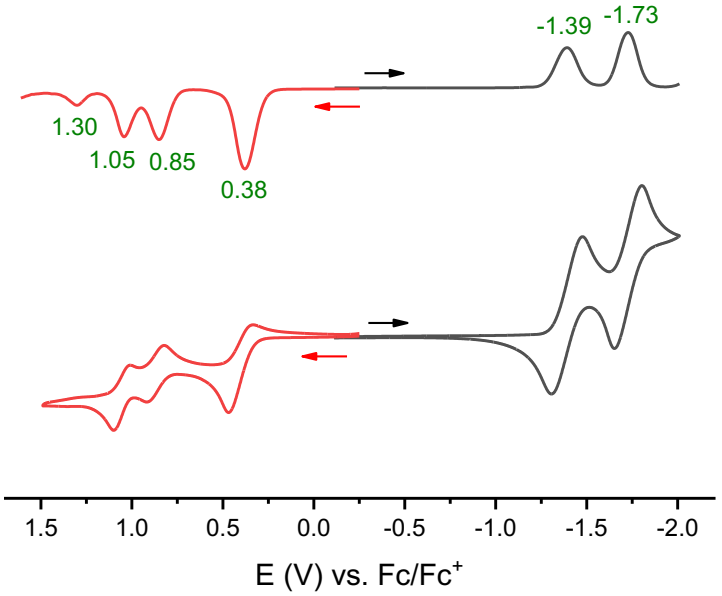

Figure S51 Cyclic (lower traces) and differential pulse (upper traces) voltammograms for **2** in dichloromethane solution. The green numbers are the electrode potentials in volts. The horizontal arrows indicate directions of the potential advances.

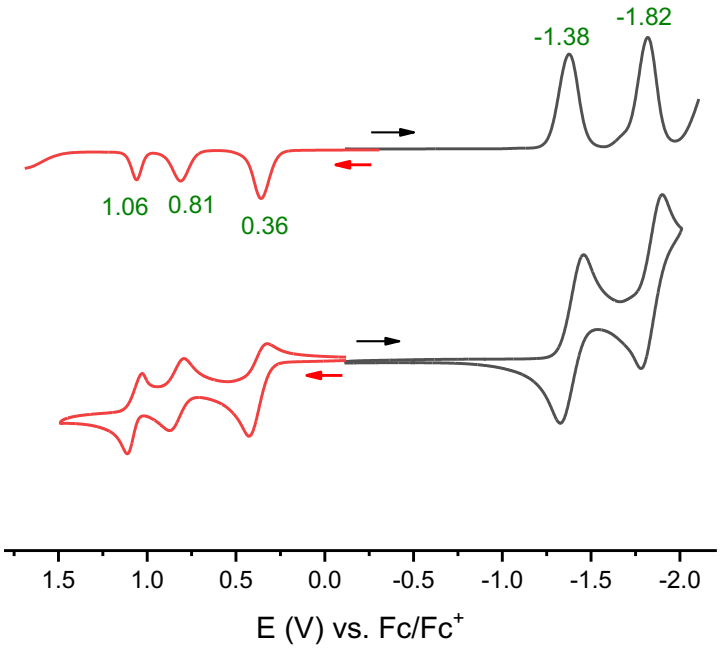

Figure S52 Cyclic (lower traces) and differential pulse (upper traces) voltammograms for **3** in dichloromethane solution. The green numbers are the electrode potentials in volts. The horizontal arrows indicate directions of the potential advances.

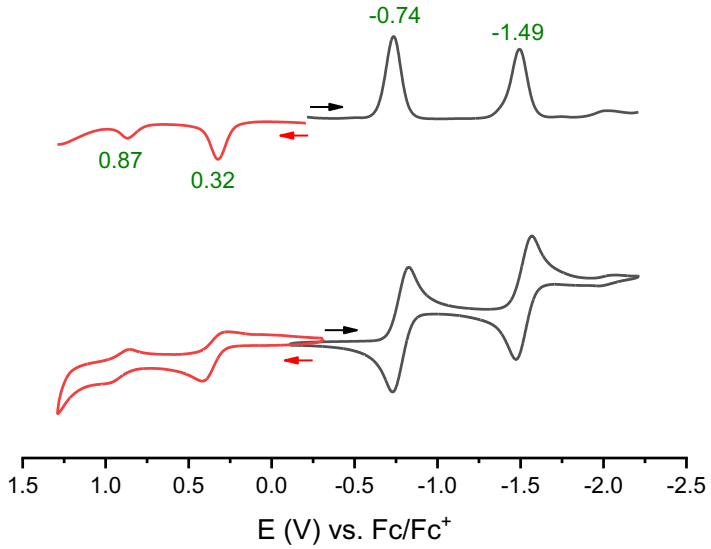

Figure S53 Cyclic (lower traces) and differential pulse (upper traces) voltammograms for **NC-1** in dichloromethane solution. The green numbers are the electrode potentials in volts. The horizontal arrows indicate directions of the potential advances.

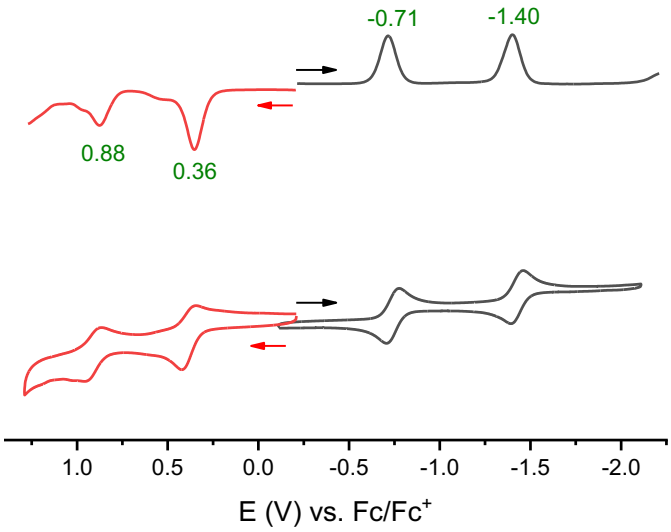

Figure S54 Cyclic (lower traces) and differential pulse (upper traces) voltammograms for **NC-2** in dichloromethane solution. The green numbers are the electrode potentials in volts. The horizontal arrows indicate directions of the potential advances.

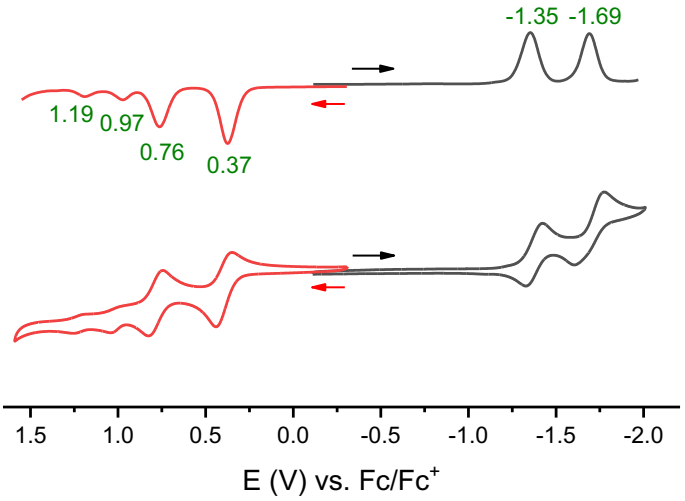

Figure S55 Cyclic (lower traces) and differential pulse (upper traces) voltammograms for **4** in dichloromethane solution. The green numbers are the electrode potentials in volts. The horizontal arrows indicate directions of the potential advances.

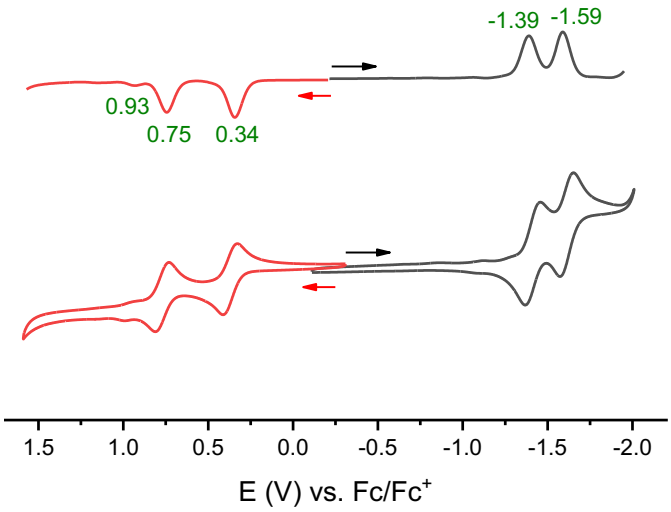

Figure S56 Cyclic (lower traces) and differential pulse (upper traces) voltammograms for **5** in dichloromethane solution. The green numbers are the electrode potentials in volts. The horizontal arrows indicate directions of the potential advances.

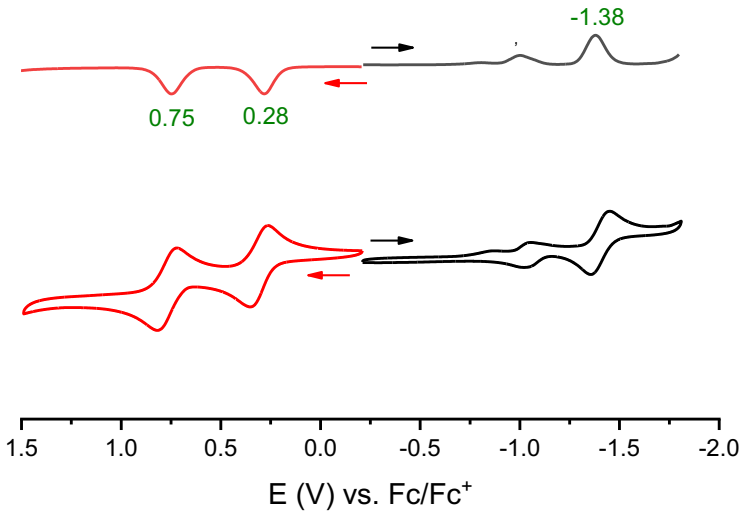

Figure S57 Cyclic (lower traces) and differential pulse (upper traces) voltammograms for **6** in dichloromethane solution. The green numbers are the electrode potentials in volts. The horizontal arrows indicate directions of the potential advances.

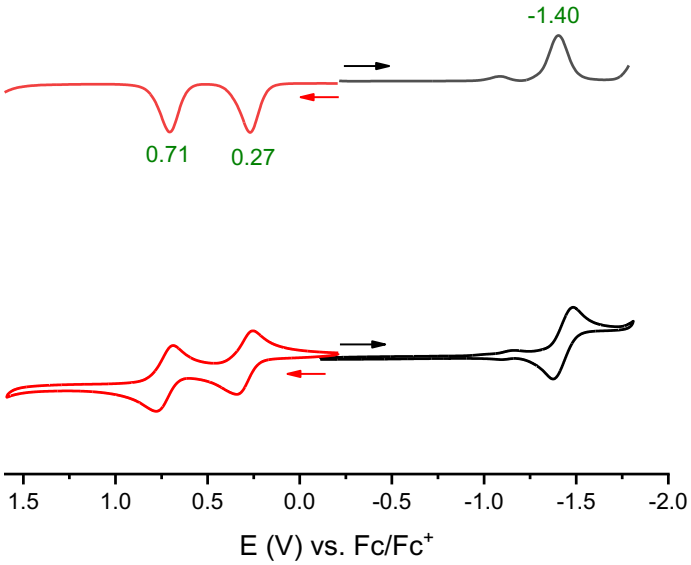

Figure S58 Cyclic (lower traces) and differential pulse (upper traces) voltammograms for **7** in dichloromethane solution. The green numbers are the electrode potentials in volts. The horizontal arrows indicate directions of the potential advances.

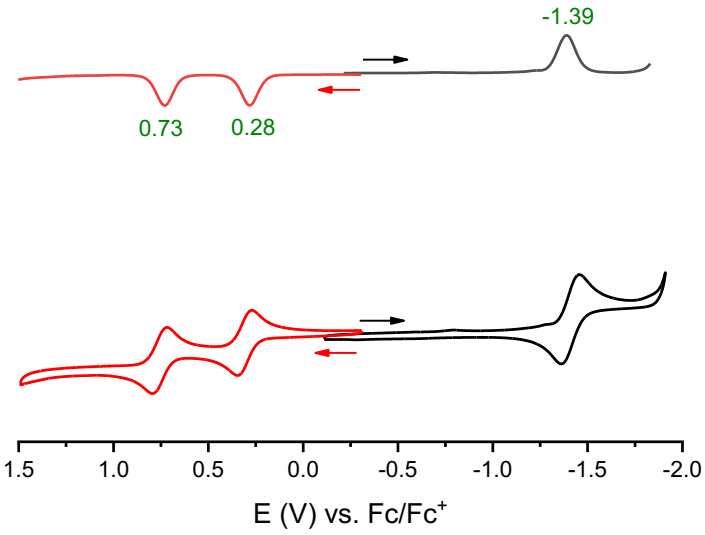

Figure S59 Cyclic (lower traces) and differential pulse (upper traces) voltammograms for **8** in dichloromethane solution. The green numbers are the electrode potentials in volts. The horizontal arrows indicate directions of the potential advances.

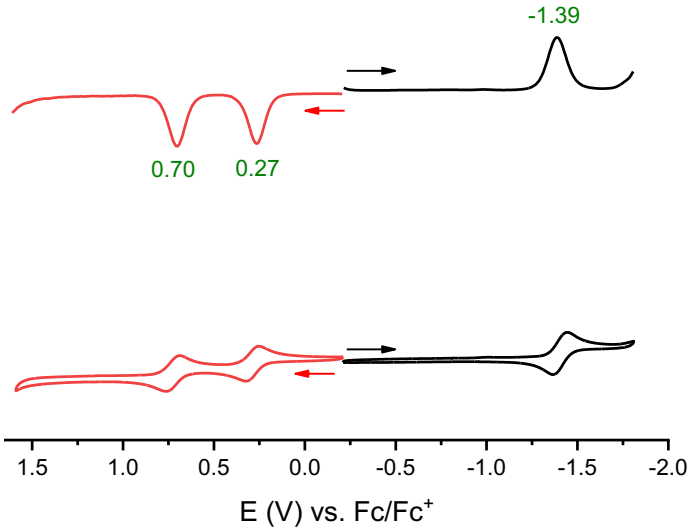

Figure S60 Cyclic (lower traces) and differential pulse (upper traces) voltammograms for **9** in dichloromethane solution. The green numbers are the electrode potentials in volts. The horizontal arrows indicate directions of the potential advances.

Table S1. Selected absorption wavelengths, energies, and oscillator strengths (*f*) of **2**, **3**, **4** and **5** calculated at the TD-B3LYP/6-31G(d)+SDD level.

Compound	State	λ [nm]	energy [eV]	*f*	Major transition
2	S_1	675.12	1.8365	0.0000	HOMO→LUMO (99.5%)
	S_2	571.08	2.1711	0.0000	HOMO–1→LUMO (99.3%)
	S_3 (Q-band)	553.86	2.2385	0.0614	HOMO–3→LUMO+1 (3.1%) HOMO–1→LUMO+2 (4.7%) HOMO→LUMO+1 (89.0%)
3	S_1	682.68	1.8161	0.0000	HOMO→LUMO (99.5%)
	S_2	578.88	2.1418	0.0001	HOMO–1→LUMO (99.3%)
	S_3 (Q-band)	537.23	2.3078	0.0636	HOMO–1→LUMO+1 (2.2%) HOMO–1→LUMO+2 (5.6%) HOMO→LUMO+1 (76.4%) HOMO→LUMO+2 (9.5%)
4	S_1	642.76	1.9289	0.0016	HOMO→LUMO (99.5%)
	S_2 (Q-band)	562.53	2.2040	0.0949	HOMO–3→LUMO+1 (3.4%) HOMO–1→LUMO (2.1%) HOMO–1→LUMO+2 (3.6%) HOMO→LUMO+1 (87.9%)
5	S_1	635.25	1.9517	0.0000	HOMO→LUMO (99.7%)
	S_2 (Q-band)	591.53	2.0960	0.0959	HOMO–3→LUMO+1 (3.2%) HOMO–1→LUMO+ (3.8%) HOMO→LUMO+1 (89.8%)

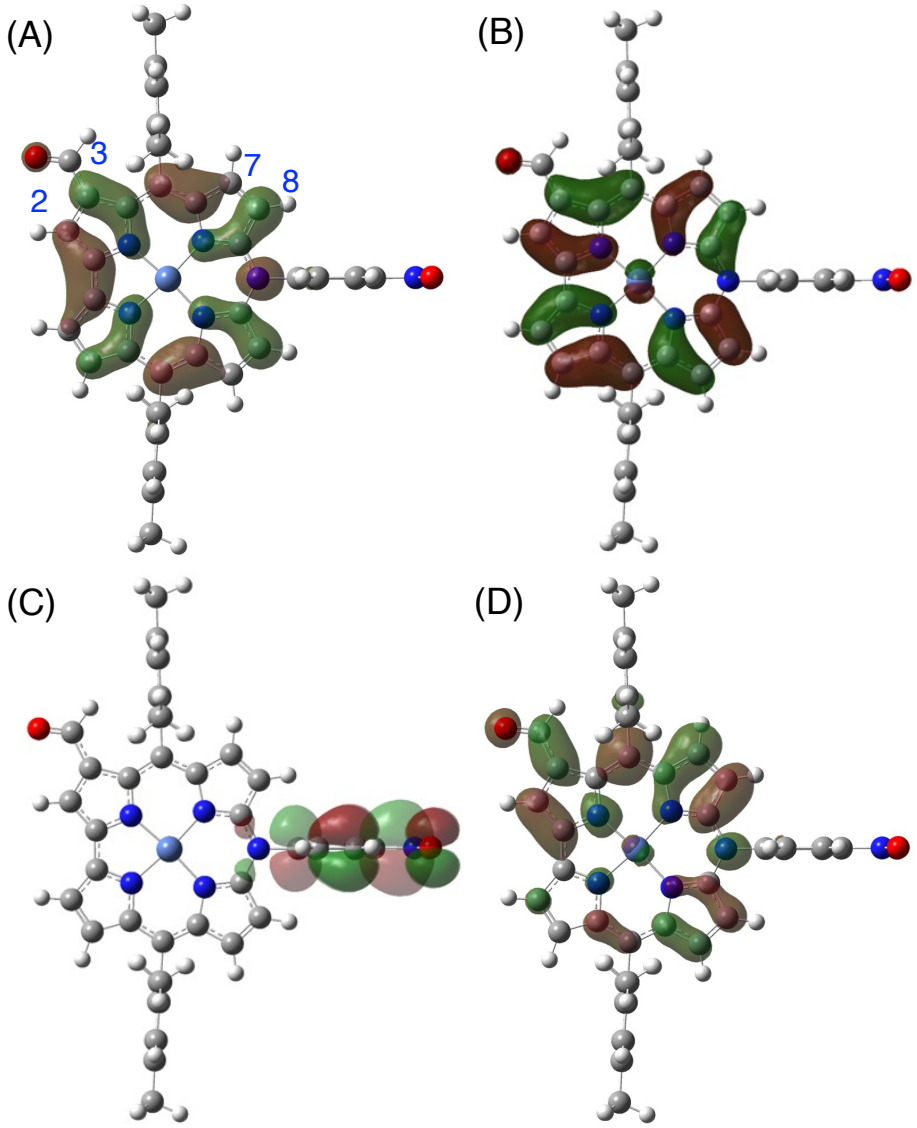

Figure S61 (A) HOMO–1, (B) HOMO, (C) LUMO and (D) LUMO+1 of azacorrole **2** calculated at the B3LYP/6-31G(d)+SDD level.

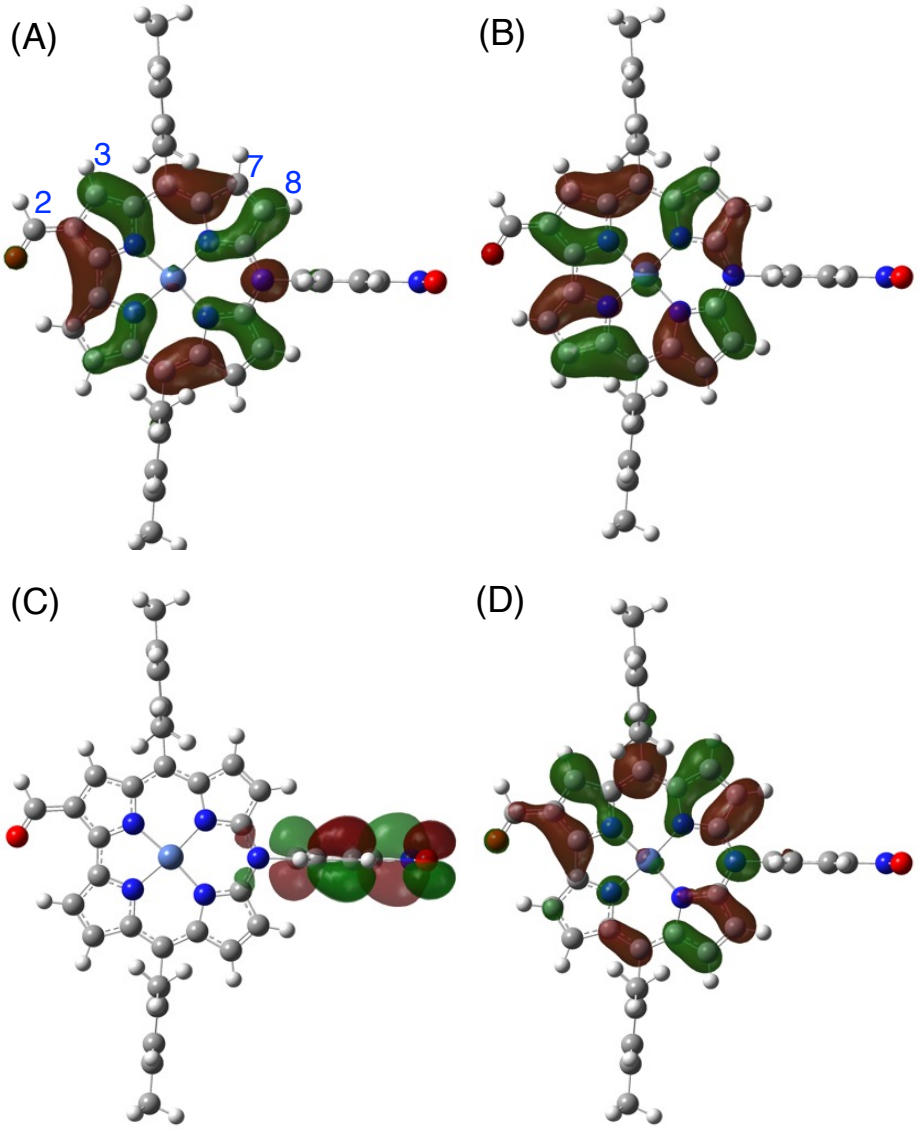

Figure S62 (A) HOMO–1, (B) HOMO, (C) LUMO and (D) LUMO+1 of azacorrole **3** calculated at the B3LYP/6-31G(d)+SDD level.

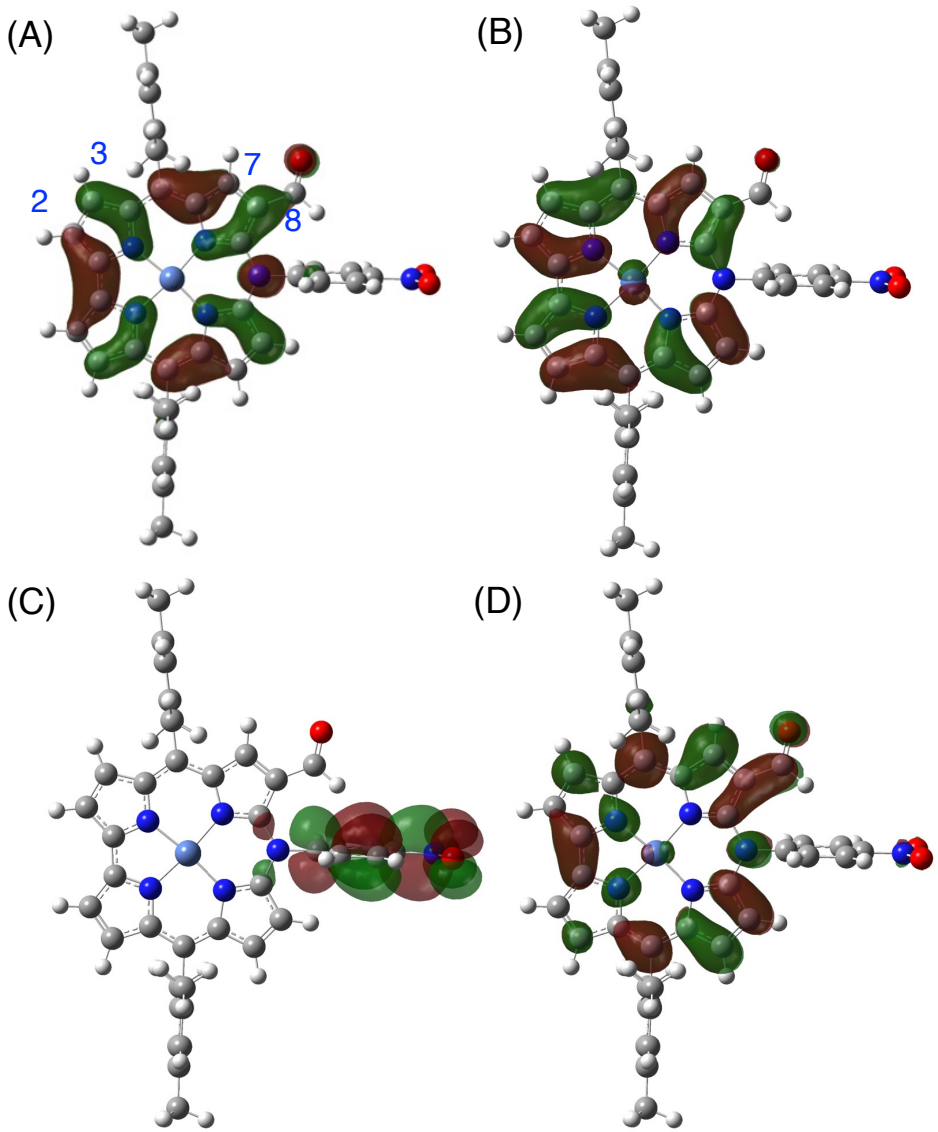

Figure S63 (A) HOMO–1, (B) HOMO, (C) LUMO and (D) LUMO+1 of azacorrole **4** calculated at the B3LYP/6-31G(d)+SDD level.

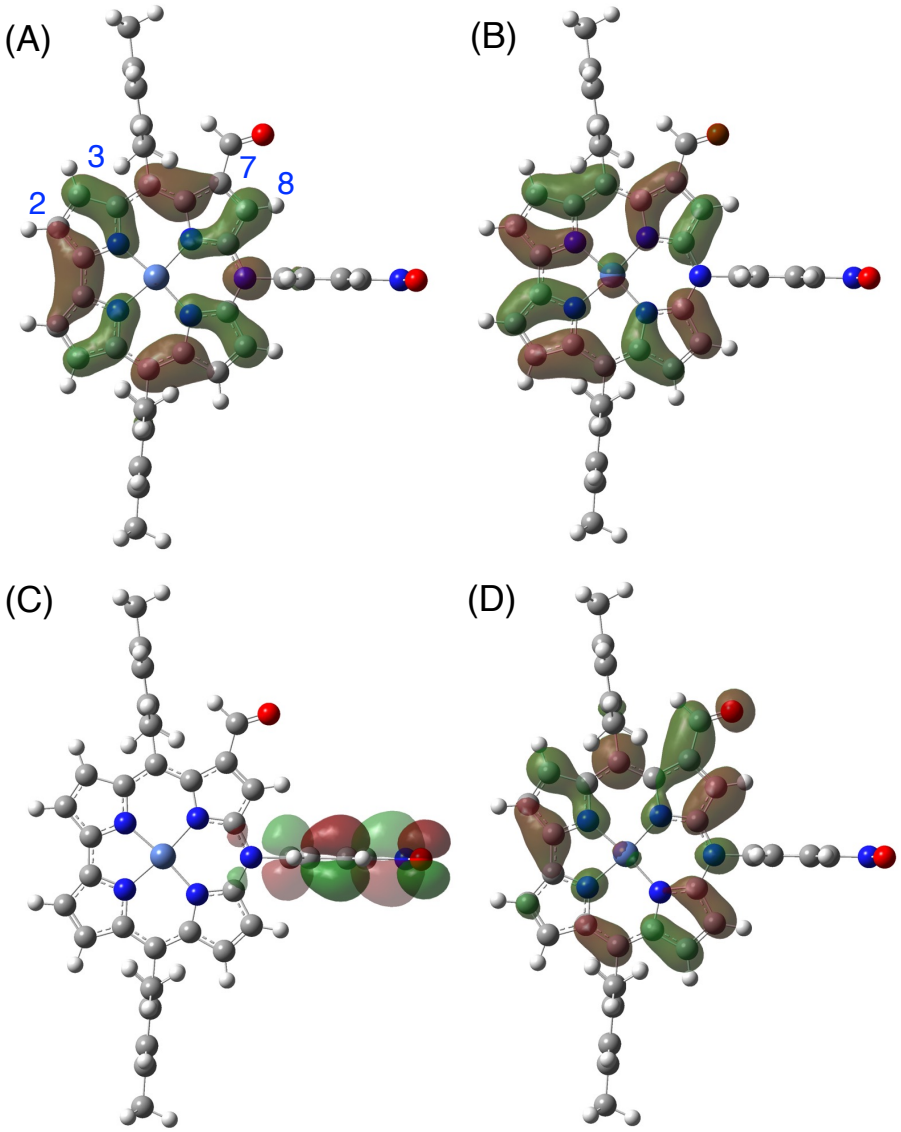

Figure S64 (A) HOMO–1, (B) HOMO, (C) LUMO and (D) LUMO+1 of azacorrole **5** calculated at the B3LYP/6-31G(d)+SDD level.